

Standard Partial Molar Volumes of Some Aqueous Alkanolamines and Alkoxyamines at Temperatures up to 325 °C: Functional Group Additivity in Polar Organic Solutes under Hydrothermal Conditions

E. Bulemela and Peter R. Tremaine*

Department of Chemistry, University of Guelph, Guelph, Ontario, Canada N1G 2W1

Received: December 14, 2007; In Final Form: January 14, 2008

Apparent molar volumes of dilute aqueous solutions of monoethanolamine (MEA), diethanolamine (DEA), triethanolamine (TEA), *N,N*-dimethylethanolamine (DMEA), ethylethanolamine (EAE), 2-diethylethanolamine (2-DEEA), and 3-methoxypropylamine (3-MPA) and their salts were measured at temperatures from 150 to 325 °C and pressures as high as 15 MPa. The results were corrected for the ionization and used to obtain the standard partial molar volumes, V_2^0 . A three-parameter equation of state was used to describe the temperature and pressure dependence of the standard partial molar volumes. The fitting parameters were successfully divided into functional group contributions at all temperatures to obtain the standard partial molar volume contributions. Including literature results for alcohols, carboxylic acids, and hydroxycarboxylic acids yielded the standard partial molar volume contributions of the functional groups $>\text{CH}-$, $>\text{CH}_2-$, $-\text{CH}_3$, $-\text{OH}$, $-\text{COOH}$, $-\text{O}-$, $>\text{N}$, $>\text{NH}$, $-\text{NH}_2$, $-\text{COO}^-\text{Na}^+$, $-\text{NH}_3^+\text{Cl}^-$, $>\text{NH}_2^+\text{Cl}^-$, and $>\text{NH}^+\text{Cl}^-$ over the range ($150\text{ °C} \leq t \leq 325\text{ °C}$). These allow predictions of the standard partial molar volume of aqueous organic solutes composed of these groups at temperatures up to $\sim 310\text{ °C}$ and pressures of 10–20 MPa to within a precision of $\pm 5\text{ cm}^3\text{mol}^{-1}$. The model could not be extended to higher temperatures because of uncertainties caused by thermal decomposition. At temperatures above $\sim 250\text{ °C}$, the order of the group contributions to V_2^0 changes from that observed at 25 °C, to become increasingly consistent with the polarity of each functional group. The effect of the dipole moment of each molecule on the contribution to V_2^0 from long-range solvent polarization was calculated from the multipole expansion of the Born equation using dipole moments estimated from restricted Hartree–Fock calculations with *Gaussian 03* (Gaussian, Inc., Wallingford, CT) and the Onsager reaction-field approximation for solvent effects. Below 325 °C, the dipole contribution was found to be less than $2\text{ cm}^3\text{mol}^{-1}$ for all the solute molecules studied. At higher temperatures and pressures near steam saturation, the effect is much larger and may explain anomalies in functional group additivity observed in small, very polar solutes.

1. Introduction

A major goal of modern physical chemistry is to extend the study of aqueous solutions to extremes of temperature and pressure. The properties of water change dramatically from subambient temperatures to conditions approaching the critical point of water at 374 °C and 22 MPa, so that measurements over wide variations of temperature and pressure provide new insights and a severe test of existing theory. Industrial and geochemical interest is centered on the need to model mass-transport, corrosion and redox mechanisms under hydrothermal conditions (100–400 °C) in a variety of man-made and natural systems where few data exist. Standard partial molar heat capacities ($C_{p,2}^0$) and volumes (V_2^0) are particularly important in this context, because they are sensitive indicators of hydration effects and yield parameters for semiempirical models used to extrapolate room-temperature data to hydrothermal conditions. Several such “equations of state” for standard partial molar properties have been reported.^{1–7} Such models are typically based on an idealized treatment of long-range solute–solvent interactions, which dominate at very high temperatures, and additional terms containing adjustable parameters to describe short-range hydration effects, which are most important near

ambient conditions. In recent years, these equations of state have been used as the basis for several functional group additivity models, which can be used to predict the standard partial molar properties of aqueous organic solutes at elevated temperatures and pressures, based on their structure.^{8–10} Because of a lack of experimental data, these models are limited to temperatures below $\sim 250\text{ °C}$. In addition, group additivity models are based on the premise that the contributions of functional group are independent of one another, and that no specific provision needs to be made for the effects of multipole moments on long-range solvent polarization. It is not yet known whether these assumptions are valid at much higher temperatures, where the dramatic increase in solvent compressibility associated with the approach to the critical point of water becomes important.

Amines, alkanolamines, and hydroxycarboxylic acids are useful model solutes for probing high temperature solvation phenomena, because they provide a direct means of examining the competing effects of ionic and uncharged functional groups. The thermal stability of some of these compounds has been quite well established from their behavior in nuclear and thermal steam generators, where they are often present as pH control agents or as contaminants. Our first such studies determined $C_{p,2}^0$ from 10 to 55 °C, and V_2^0 at temperatures up to 300 °C, for aqueous morpholine,¹¹ dimethylamine (DMA),¹² methyl-dietha-

* Corresponding author. E-mail: tremaine@uoguelph.ca.

nolamine (MDEA),¹³ and their chloride salts. The standard partial molar volumes for all these solutes approach large positive values at elevated temperatures, consistent with a lowering of the critical temperature in the solutions relative to water, and the effect in the chloride salts is reversed. Such behavior is formally described by the Krichevskii parameter,^{14,15} which describes the limiting behavior of dilute solutions as they approach the critical point of pure water, and the positive or negative divergence of $C_{p,2}^0$ and V_2^0 at the critical point. The sign of the Krichevskii parameter is determined by the relative strength of solute–solvent and solvent–solvent interactions. Our most recent work has extended these studies to simple amino acids^{16,17} and hydroxycarboxylic acids with closely packed polar groups in an attempt to examine the limiting high-temperature behavior of very polar neutral species, and the competition between hydrophobic and hydrophilic interactions.

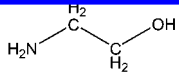
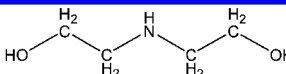
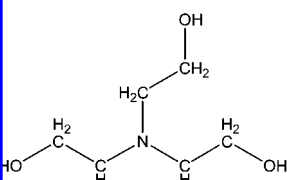
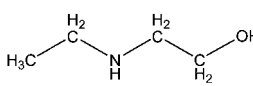
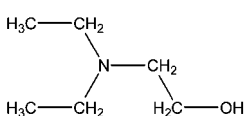
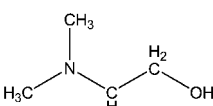
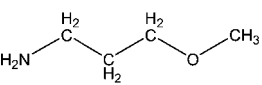
The objective of the present work is to extend these studies further, by measuring standard partial molar volumes for solutes containing most of the common functional groups, up to temperatures well above 250 °C, the limit of current functional group additivity models. We particularly seek to reach temperatures above 300 °C, where long-range polarization effects become increasingly important and the behavior of V_2^0 is expected to reflect the near-critical Krichevskii limit. In selecting thermally stable solute candidates for study, we have been guided by the work of P.V. Balakrishnan at Chalk River Nuclear Laboratories,¹⁸ who determined equilibrium constants for a number of thermally stable amines, alkanolamines, and alkoxyamines of interest to the nuclear industry for use at temperatures up to 300 °C as pH control agents. These compounds include many of the functional groups required for our study, and the availability of experimental ionization constants is required for data analysis. The seven solute molecules selected for our study are: monoethanolamine (MEA), diethanolamine (DEA), triethanolamine (TEA), *N,N*-dimethylethanolamine (DMEA), ethylethanolamine (EAE), 2-diethylethanolamine (2-DEEA), and 3-methoxypropylamine (3-MPA). Their structures are depicted in Table 1. Together with recently published volumetric data for carboxylic acids and alcohols^{19,20} and our own earlier work, the resulting data base contains values for enough functional group combinations assess the contribution of individual groups and to develop a primitive group additivity model.

This paper describes the measurements of apparent molar volumes of the seven alkanolamines and one alkoxyamine noted above at temperatures between 150 °C $\leq t \leq$ 325 °C and pressures up to 15 MPa. The contributions to V_2^0 associated with their constituent functional groups have been assessed as a function of temperature and pressure and used as the basis for a simple group additivity model. Our treatment includes an evaluation of the magnitude of long-range polarization at very high temperatures to assess multipole solvation effects.

2. Experimental Section

Monoethanolamine [$\text{H}_2\text{N}(\text{C}_2\text{H}_4\text{OH})$, 99+%], diethanolamine [$\text{HN}(\text{C}_2\text{H}_4\text{OH})_2$, 99%], triethanolamine [$\text{N}(\text{C}_2\text{H}_4\text{OH})_3$, 98%], *N,N*-dimethylethanolamine [$(\text{CH}_3)_2\text{N}(\text{C}_2\text{H}_4\text{OH})$, 99.5+%], 2-diethylethanolamine [$(\text{C}_2\text{H}_5)_2\text{N}(\text{C}_2\text{H}_4\text{OH})$, 99.5+%], and 3-methoxypropylamine [$\text{H}_2\text{N}(\text{CH}_2)_3\text{OCH}_3$, 99%] were from Aldrich Chemical Co., and ethylethanolamine [$\text{C}_2\text{H}_5\text{NH}(\text{C}_2\text{H}_4\text{OH})$, 99+%] was from Acros Organics. These compounds were used as received after confirmatory analysis with standard hydro-

TABLE 1: Molecular Structures of Alkanolamines and Alkoxyamine Studied in This Work

	
Monoethanolamine (MEA)	Diethanolamine (DEA)
	
Triethanolamine (TEA)	Ethylethanolamine (EAE)
	
2-Diethylethanolamine (2-DEEA)	<i>N,N</i> -Dimethylethanolamine (DMEA)
	
3-Methoxypropylamine (3-MPA)	

chloric acid (Fisher Scientific, certified A.C.S., 36.5–38.0%). The HCl solution was standardized by titration against tris-(hydroxymethyl) aminomethane (Aldrich, 99.9%) which had been previously dried to constant mass at 110 °C. Nanopure water (resistivity 18.2 MΩ·cm), degassed by boiling, was used to prepare aqueous amine solutions. Solutions of the amines with water were made by mass with care being taken to minimize exposure to air (carbon dioxide). The estimated uncertainty in the molalities was within $\pm 0.2\%$. Stock solutions of chloride salts of the amines were prepared by adding a weighed amount of standard HCl to the stock solutions of neutral amine (R_3N) in excess of the amine by about 1 mol percent, so as to suppress the hydrolysis of $\text{R}_3\text{NH}^+\text{Cl}^-$ by maintaining acidic conditions.¹³ The presence of oxygen/air in the flow system was minimized by using freshly boiled Nanopure water in the HPLC syringe pump. All solutions were stored in sealed containers and further degassed by suction in a sealed syringe immediately prior to injection into the loop.

High-temperature volumetric measurements were made in a vibrating-tube densitometer, constructed according to the design of Albert and Wood,²¹ as modified by Corti et al.²² A detailed description of the densitometer and experimental procedures has been given by Xiao et al.²³ and Clarke and Tremaine.¹⁶ In this study, measurements were carried out at temperatures from 150 to 325 °C and at constant pressures in excess of steam saturation, $p = 11$ MPa and $p = 15$ MPa, as appropriate. The densitometer was calibrated daily with pure water and a standard solution of 1.1067 mol·kg⁻¹ NaCl (aq), using the reference values compiled by Hill²⁴ and Archer,²⁵ respectively. The combined uncertainty in the measured relative densities, $(\rho - \rho_1^*)$, due to the sensitivity limits of the instrument itself and the accuracy of the reference data, is estimated to be ± 0.0002 g·cm⁻³. The precision is ± 0.00002 g·cm⁻³. Temperature was controlled within ± 0.1 °C and pressure to within ± 0.1 MPa.

Our interest was to obtain as many data as possible for use in examining the applicability of existing group additivity estimation methods at temperatures above their current limit of

TABLE 2: Apparent Molar Volume $V_{\phi,2}$ for Aqueous Ethylaminoethanol (EAE) after the Degree of Dissociation Correction

t °C	p MPa	m_2 mol·kg ⁻¹	$10^2 \cdot (\rho - \rho_1^*)$ g·cm ⁻³	V_{ϕ}^{exp} cm ³ ·mol ⁻¹	α	$V_{\phi,2}$ cm ³ ·mol ⁻¹
$t = (150.87 \pm 0.03)^\circ\text{C}; p = (15.24 \pm 0.01) \text{ MPa}$						
150.84	15.26	1.0299	0.6248	104.23	0.0069	104.35 ± 0.01
150.82	15.25	0.7994	0.4889	104.13	0.0078	104.27 ± 0.01
150.87	15.24	0.6460	0.4034	104.19	0.0087	104.35 ± 0.01
150.91	15.24	0.4211	0.2621	104.01	0.0108	104.21 ± 0.01
150.89	15.23	0.3193	0.1848	103.41	0.0124	103.63 ± 0.02
150.87	15.24	0.2252	0.1300	103.33	0.0147	103.59 ± 0.02
$t = (200.72 \pm 0.01)^\circ\text{C}; p = (15.25 \pm 0.02) \text{ MPa}$						
200.72	15.24	1.0299	0.7525	112.53	0.0044	112.65 ± 0.03
200.72	15.24	0.7994	0.5854	112.34	0.0050	112.47 ± 0.02
200.72	15.23	0.6460	0.4825	112.40	0.0056	112.55 ± 0.02
200.72	15.24	0.4211	0.3082	111.98	0.0069	112.15 ± 0.02
200.72	15.28	0.3193	0.2380	112.06	0.0080	112.27 ± 0.02
200.73	15.25	0.2252	0.1664	111.88	0.0095	112.13 ± 0.02
$t = (250.32 \pm 0.03)^\circ\text{C}; p = (15.24 \pm 0.01) \text{ MPa}$						
250.27	15.22	1.0299	0.9010	124.60	0.0024	124.72 ± 0.04
250.32	15.25	0.7994	0.7174	124.67	0.0027	124.80 ± 0.05
250.35	15.23	0.6460	0.5883	124.68	0.0030	124.83 ± 0.04
250.34	15.24	0.4211	0.3748	124.03	0.0037	124.22 ± 0.04
250.32	15.22	0.3193	0.2923	124.29	0.0042	124.51 ± 0.04
$t = (275.23 \pm 0.01)^\circ\text{C}; p = (15.26 \pm 0.02) \text{ MPa}$						
275.23	15.24	1.0299	1.0341	134.06	0.0016	134.19 ± 0.04
275.23	15.25	0.7994	0.8368	134.43	0.0018	134.57 ± 0.04
275.22	15.29	0.6460	0.6776	134.18	0.0020	134.34 ± 0.04
275.22	15.25	0.4211	0.4629	134.66	0.0024	134.86 ± 0.04
275.22	15.26	0.3193	0.3702	135.51	0.0028	135.74 ± 0.03
$t = (300.18 \pm 0.03)^\circ\text{C}; p = (15.25 \pm 0.01) \text{ MPa}$						
300.23	15.25	1.0299	1.2946	149.37	0.0011	149.53 ± 0.06
300.17	15.25	0.7994	1.0974	151.16	0.0012	151.34 ± 0.06
300.16	15.25	0.6460	0.9428	152.50	0.0014	152.70 ± 0.04
300.16	15.26	0.4211	0.6736	154.61	0.0017	154.86 ± 0.03
300.16	15.26	0.3193	0.5298	155.44	0.0020	155.73 ± 0.04
$t = (325.13 \pm 0.02)^\circ\text{C}; p = (15.26 \pm 0.01) \text{ MPa}$						
325.13	15.26	1.0299	2.2219	188.99	0.0008	189.21 ± 0.22
325.11	15.25	0.7994	1.9096	193.43	0.0009	193.68 ± 0.12
325.13	15.26	0.6460	1.5088	191.03	0.0010	191.31 ± 0.12
325.12	15.26	0.4211	1.0386	192.66	0.0012	193.00 ± 0.11
325.14	15.25	0.3193	0.7513	189.25	0.0014	189.64 ± 0.17
325.15	15.26	0.2252	0.5816	194.01	0.0017	194.48 ± 0.11

250 °C. In the initial phase of this study, the relative densities of solutions of EAE (aq), 2-DEEA(aq), and 3-MPA-(aq) were measured over the molality range $0.1 < m/(\text{mol}\cdot\text{kg}^{-1}) < 1$. The resulting apparent molar volumes for these neutral species, calculated from these values of $(\rho - \rho_1^*)$, showed no statistically significant molality dependence. The latter part of the program followed the procedure used by Criss and Wood⁸ in which the apparent molar volumes for other neutral species, MEA(aq), DEA(aq), TEA(aq), and DMEA(aq), were determined from replicate measurements of $(\rho - \rho_1^*)$ at one concentration, $m \approx 0.5 \text{ mol}\cdot\text{kg}^{-1}$. Apparent molar volumes for the salts were determined over the range 0.2–1 mol·kg⁻¹.

Because the objective of this work was to determine standard partial molar volumes at the highest achievable temperatures, it was critically important to identify the onset of thermal decomposition. As in our previous work,^{26,27} a liquid chromatography loop was used to collect solution samples immediately after they had passed through the densimeter. ¹³C NMR analysis was used to examine solutions of the neutral species for thermal decomposition products (detection limit ~2%). The ¹³C NMR spectra showed extra peaks corresponding to decomposition products for MEA, DEA, TEA, DMEA, EAE, and 3-MPA at 350 °C and 2-DEEA at 325 °C. Because the spectra were obtained at ambient pressure, volatile decomposition products

TABLE 3: Apparent Molar Volume $V_{\phi,2}$ for Aqueous 2-Diethylethanolamine (2-DEEA) after the Degree of Dissociation Correction

t °C	p MPa	m_2 mol·kg ⁻¹	$10^2 \cdot (\rho - \rho_1^*)$ g·cm ⁻³	V_{ϕ}^{exp} cm ³ ·mol ⁻¹	α	$V_{\phi,2}$ cm ³ ·mol ⁻¹
$t = (149.54 \pm 0.40)^\circ\text{C}; p = (15.41 \pm 0.01) \text{ MPa}$						
149.09	15.42	1.0114	1.0863	140.71	0.0087	140.86 ± 0.05
149.16	15.41	0.7942	0.8703	140.65	0.0098	140.82 ± 0.05
149.37	15.42	0.6066	0.6431	139.91	0.0112	140.10 ± 0.06
149.64	15.40	0.4171	0.4704	140.49	0.0134	140.72 ± 0.04
149.90	15.42	0.3032	0.3449	140.45	0.0157	140.72 ± 0.03
150.05	15.42	0.1985	0.2138	139.56	0.0194	139.88 ± 0.04
$t = (199.19 \pm 0.03)^\circ\text{C}; p = (15.39 \pm 0.01) \text{ MPa}$						
199.26	15.39	1.0114	1.3791	154.03	0.0050	154.19 ± 0.11
199.19	15.40	0.7942	1.0978	153.76	0.0057	153.93 ± 0.07
199.18	15.41	0.6066	0.8735	154.12	0.0065	154.32 ± 0.07
199.17	15.39	0.4171	0.5763	152.83	0.0078	153.06 ± 0.06
199.16	15.39	0.3032	0.4169	152.46	0.0092	152.73 ± 0.08
199.19	15.40	0.1985	0.3042	154.33	0.0113	154.68 ± 0.08
$t = (249.22 \pm 0.03)^\circ\text{C}; p = (15.39 \pm 0.02) \text{ MPa}$						
249.21	15.40	1.0114	1.8130	175.25	0.0028	175.42 ± 0.14
249.23	15.37	0.7942	1.4696	175.40	0.0032	175.59 ± 0.10
249.24	15.43	0.6066	1.1326	174.91	0.0036	175.13 ± 0.10
249.24	15.39	0.4171	0.8021	175.05	0.0044	175.32 ± 0.10
249.17	15.38	0.3032	0.5955	175.21	0.0051	175.52 ± 0.09
$t = (275.42 \pm 0.10)^\circ\text{C}; p = (15.32 \pm 0.01) \text{ MPa}$						
275.55	15.32	0.8538	1.9604	195.34	0.0021	195.53 ± 0.09
275.51	15.33	0.8108	1.8560	194.93	0.0021	195.12 ± 0.09
275.33	15.31	0.3806	0.9727	197.12	0.0031	197.41 ± 0.06
275.34	15.31	0.3060	0.7984	197.57	0.0035	197.90 ± 0.04
275.38	15.32	0.2314	0.5850	195.68	0.0040	196.05 ± 0.05
$t = (300.34 \pm 0.03)^\circ\text{C}; p = (15.31 \pm 0.01) \text{ MPa}$						
300.36	15.31	0.8538	2.5528	226.29	0.0013	226.49 ± 0.15
300.40	15.31	0.8108	2.4333	226.16	0.0013	226.36 ± 0.12
300.32	15.31	0.5946	1.8927	227.92	0.0015	228.15 ± 0.07
300.30	15.31	0.3806	1.3417	232.75	0.0019	233.06 ± 0.14
300.34	15.33	0.3060	1.1162	234.40	0.0022	234.75 ± 0.12
300.35	15.31	0.2314	0.8966	238.07	0.0025	238.48 ± 0.10

such as NH₃(g) would not be detected by NMR. The analyses for thermal decomposition of the salts of these species was carried out by both ¹³C and ¹H NMR. The NMR spectra showed that significant thermal decomposition of all the salts took place at 325 °C.

Quantum mechanical calculations were performed with the *Gaussian 03* program (Gaussian Inc., Wallingford, CT) at the restricted Hartree–Fock level of theory, using a full geometry optimization with the 6-31G(d, p) basis set. Details are discussed in Section 5.

3. Results

3.1. Standard Partial Molar Volumes. The relative density of solutions in the vibrating-tube densitometer was determined from the expression

$$\rho - \rho_1^* = K(\tau^2 - \tau_1^2) \quad (1)$$

where ρ and ρ_1^* are the densities of the solution and the water, respectively, τ and τ_1 are the resonance periods of the solution and water, respectively, and K is a characteristic constant determined by calibration with water and the standard NaCl solution at each temperature and pressure. The experimental apparent molar volumes, V_{ϕ}^{exp} were calculated from the density data using the usual expression in SI units

$$V_{\phi}^{\text{exp}} = (\rho_1^* - \rho)/(m\rho\rho_1^*) + M/\rho \quad (2)$$

where ρ_1^* and ρ are the densities of pure water and solution in kg·m⁻³ (1 g·cm⁻³ = 1000 kg·m⁻³), respectively, m is the

TABLE 4: Apparent Molar Volume $V_{\phi,2}$ for Aqueous 3-Methoxypropylamine (3-MPA) after the Degree of Dissociation Correction

t °C	p MPa	m_2 mol·kg ⁻¹	$10^2 \cdot (\rho - \rho_1^*)$ g·cm ⁻³	V_{ϕ}^{exp} cm ³ ·mol ⁻¹	α	$V_{\phi,2}$ cm ³ ·mol ⁻¹
$t = (149.23 \pm 0.05)^\circ\text{C}; p = (15.29 \pm 0.01) \text{ MPa}$						
149.27	15.30	1.1580	1.0378	107.94	0.0046	108.03 ± 0.10
149.27	15.30	0.8087	0.7485	107.94	0.0055	108.05 ± 0.12
149.25	15.29	0.6562	0.6251	108.12	0.0062	108.24 ± 0.09
149.21	15.28	0.4265	0.3982	107.62	0.0076	107.77 ± 0.09
149.16	15.30	0.2929	0.2937	108.30	0.0092	108.49 ± 0.09
$t = (200.78 \pm 0.03)^\circ\text{C}; p = (15.24 \pm 0.01) \text{ MPa}$						
200.79	15.25	1.0075	1.0813	117.51	0.0030	117.61 ± 0.04
200.79	15.24	0.7924	0.8605	117.39	0.0034	117.50 ± 0.04
200.75	15.24	0.6008	0.6509	117.06	0.0039	117.19 ± 0.04
200.75	15.25	0.4079	0.4459	116.91	0.0048	117.06 ± 0.04
200.82	15.23	0.3331	0.3525	116.34	0.0053	116.51 ± 0.04
$t = (246.51 \pm 0.06)^\circ\text{C}; p = (15.31 \pm 0.01) \text{ MPa}$						
246.49	15.32	1.1580	1.3703	129.10	0.0014	129.18 ± 0.10
246.54	15.30	0.8087	0.9818	128.95	0.0017	129.05 ± 0.08
246.56	15.30	0.6562	0.7921	128.55	0.0019	128.66 ± 0.09
246.54	15.29	0.4265	0.5067	127.81	0.0023	127.95 ± 0.09
246.51	15.32	0.2929	0.3540	127.87	0.0028	128.03 ± 0.10
246.40	15.30	0.1949	0.2455	128.44	0.0034	128.65 ± 0.04
$t = (275.29 \pm 0.03)^\circ\text{C}; p = (15.26 \pm 0.01) \text{ MPa}$						
275.26	15.26	1.0075	1.3357	140.09	0.0008	140.16 ± 0.06
275.25	15.26	0.7924	1.0797	140.24	0.0009	140.32 ± 0.06
275.30	15.28	0.6008	0.8364	140.31	0.0011	140.41 ± 0.04
275.31	15.26	0.4079	0.5851	140.58	0.0013	140.69 ± 0.04
275.32	15.26	0.3331	0.4725	140.10	0.0014	140.23 ± 0.03
$t = (299.97 \pm 0.03)^\circ\text{C}; p = (15.30 \pm 0.01) \text{ MPa}$						
299.95	15.31	1.1580	1.7332	154.78	0.0010	154.92 ± 0.09
299.98	15.31	0.8087	1.2483	154.65	0.0012	154.82 ± 0.07
300.02	15.31	0.6562	1.0281	154.64	0.0013	154.83 ± 0.04
299.94	15.29	0.4265	0.7047	155.55	0.0016	155.78 ± 0.10
299.95	15.29	0.2929	0.4945	155.80	0.0020	156.07 ± 0.08
$t = (325.41 \pm 0.02)^\circ\text{C}; p = (15.31 \pm 0.01) \text{ MPa}$						
325.42	15.32	1.1580	2.5852	192.07	0.0008	192.27 ± 0.15
325.41	15.32	0.8087	2.0381	197.14	0.0009	197.39 ± 0.11
325.39	15.31	0.6562	1.8130	202.08	0.0010	202.36 ± 0.16
325.40	15.31	0.4265	1.3797	211.65	0.0012	212.01 ± 0.15
325.43	15.31	0.2929	0.9252	208.45	0.0015	208.88 ± 0.16
325.43	15.31	0.1949	0.6542	212.14	0.0018	212.68 ± 0.09
$t = (340.26 \pm 0.04)^\circ\text{C}; p = (16.95 \pm 0.01) \text{ MPa}$						
340.28	16.94	1.1580	3.8423	243.80	0.0006	244.06 ± 0.40
340.28	16.94	0.8087	3.0133	251.47	0.0008	251.79 ± 0.17
340.30	16.96	0.6562	2.7723	263.90	0.0008	264.26 ± 0.36
340.22	16.95	0.4265	2.2056	286.52	0.0011	287.00 ± 0.30
340.21	16.96	0.2929	1.5900	290.35	0.0013	290.94 ± 0.24

solution molality (mol·kg⁻¹), and M is the molar mass of solute (kg·mol⁻¹). The experimentally determined relative densities ($\rho - \rho_1^*$) and apparent molar volumes are listed in Tables 2 to 5. A typical plot of V_{ϕ}^{exp} against molality is shown in Figure 1. The uncertainties in V_{ϕ}^{exp} were estimated from the expression given in our previous work.²⁷ These include the random errors that originate from the scatter associated with the density measurements, as well as systematic errors estimated from uncertainties in determining the temperatures, pressures, and calibration constant. The estimated accuracy of $\pm 0.0002 \text{ g}\cdot\text{cm}^{-3}$ in relative density corresponds to less than $\pm 1 \text{ cm}^3\cdot\text{mol}^{-1}$ in V_{ϕ}^{exp} at all temperatures. The statistical uncertainty in V_{ϕ}^{exp} for the chloride salts varied and was found to increase with temperature from typical values of $\pm 0.02 \text{ cm}^3\cdot\text{mol}^{-1}$ or less below 250 °C, rising to $\pm 0.30 \text{ cm}^3\cdot\text{mol}^{-1}$ at the highest temperatures studied. The statistical uncertainty in molality is the main contributor, while the uncertainties in temperature and pressure were found to be negligible. The possibility of systematic errors from undetected thermal decomposition is discussed later in this section.

The nominal apparent molar volume, V_{ϕ}^{exp} , resulting from experimental measurements on amines is the sum of contribu-

TABLE 5: Apparent Molar Volume $V_{\phi,2}$ for Other Aqueous Alkanolamines at $m = 0.5 \text{ mol}\cdot\text{kg}^{-1}$ after the Degree of Dissociation Correction

t °C	p MPa	m_2 mol·kg ⁻¹	$10^2 \cdot (\rho - \rho_1^*)$ g·cm ⁻³	V_{ϕ}^{exp} cm ³ ·mol ⁻¹	α	$V_{\phi,2}$ cm ³ ·mol ⁻¹
monoethanolamine (MEA)						
150.30	15.18	0.4940	-0.0399	65.00	0.0054	65.11 ± 0.01
150.30	15.17	0.5016	-0.0775	64.11	0.0054	64.22 ± 0.01
200.37	15.17	0.4940	-0.0642	68.14	0.0037	68.27 ± 0.02
200.34	15.18	0.5016	-0.0871	67.56	0.0036	67.68 ± 0.03
250.07	15.18	0.4940	-0.0943	71.86	0.0021	72.00 ± 0.03
250.15	15.19	0.5016	-0.0552	73.12	0.0021	73.25 ± 0.02
300.21	15.16	0.4940	-0.0332	82.78	0.0010	82.92 ± 0.04
300.27	15.18	0.5016	-0.0508	82.12	0.0010	82.27 ± 0.04
325.14	15.18	0.4940	0.3097	106.56	0.0010	106.85 ± 0.07
325.12	15.18	0.5016	0.3072	106.22	0.0009	106.51 ± 0.11
diethanolamine (DEA)						
150.36	15.20	0.4976	-0.4907	101.51	0.0050	101.61 ± 0.04
150.38	15.19	0.4999	-0.4881	101.63	0.0050	101.72 ± 0.04
200.38	15.18	0.4976	-0.4842	106.98	0.0033	107.09 ± 0.04
200.35	15.17	0.4999	-0.5043	106.49	0.0033	106.59 ± 0.03
250.11	15.19	0.4976	-0.4872	113.42	0.0020	113.54 ± 0.05
250.12	15.18	0.4999	-0.4994	113.11	0.0020	113.23 ± 0.04
300.22	15.17	0.4976	-0.4970	124.99	0.0011	125.15 ± 0.09
300.24	15.18	0.4999	-0.4888	125.38	0.0011	125.54 ± 0.06
325.11	15.18	0.4976	-0.2804	144.78	0.0008	145.02 ± 0.16
325.12	15.20	0.4999	-0.3162	143.15	0.0008	143.39 ± 0.18
triethanolamine (TEA)						
150.44	15.19	0.4937	-0.8574	139.57	0.0016	139.60 ± 0.08
150.50	15.18	0.4983	-0.8632	139.61	0.0016	139.64 ± 0.08
200.40	15.18	0.4937	-0.8668	146.29	0.0012	146.33 ± 0.07
200.36	15.17	0.4983	-0.8762	146.23	0.0012	146.26 ± 0.07
250.19	15.16	0.4937	-0.8749	154.49	0.0008	154.54 ± 0.09
250.16	15.19	0.4983	-0.8924	154.16	0.0008	154.20 ± 0.09
300.27	15.18	0.4937	-0.9133	168.22	0.0005	168.28 ± 0.14
300.23	15.17	0.4983	-0.9673	166.38	0.0005	166.44 ± 0.13
325.19	15.17	0.4937	-0.8242	184.35	0.0004	184.43 ± 0.29
325.22	15.17	0.4983	-0.7852	186.57	0.0004	186.65 ± 0.31
<i>N,N</i> -dimethylethanolamine (DMEA)						
150.93	15.14	0.4976	0.3716	105.40	0.0115	105.64 ± 0.03
150.87	15.63	0.5011	0.3711	105.32	0.0115	105.56 ± 0.03
200.62	15.15	0.4976	0.4451	114.31	0.0110	114.72 ± 0.02
200.58	15.14	0.5011	0.4429	114.15	0.0109	114.56 ± 0.02
250.49	15.14	0.4976	0.5422	126.37	0.0095	127.02 ± 0.03
250.47	15.16	0.5011	0.5453	126.32	0.0095	126.98 ± 0.04
275.35	15.12	0.4976	0.6281	137.74	0.0087	138.65 ± 0.03
275.35	15.14	0.5011	0.6345	137.82	0.0086	138.72 ± 0.03
300.34	15.13	0.4976	0.7526	152.98	0.0079	154.28 ± 0.04
300.29	15.12	0.5011	0.7819	153.95	0.0078	155.25 ± 0.06
325.23	15.13	0.4976	1.2099	192.60	0.0071	194.89 ± 0.17
325.22	15.13	0.5011	1.1946	191.47	0.0071	193.74 ± 0.22

tions of undissociated and ionized species formed by hydrolysis, according to reactions of the type



The contributions of the ionic species were subtracted using Young's rule,²⁸ where

$$V_{\phi}^{\text{exp}} = (1 - \alpha) V_{\phi,2}(\text{R}_3\text{N}, \text{aq}) - \alpha V_{\phi,2}(\text{H}_2\text{O}, \text{l}) + \alpha V_{\phi,2}(\text{R}_3\text{NH}^+, \text{aq} + \text{Cl}^-, \text{aq}) - \alpha V_{\phi,2}(\text{Cl}^-, \text{aq}) + \alpha V_{\phi,2}(\text{OH}^-, \text{aq}) \quad (4)$$

The degree of ionization, α , was evaluated from ionization constants reported in the literature.¹⁸ To the accuracy required here, values for $V_{\phi,2}(\text{R}_3\text{NH}^+, \text{aq} + \text{Cl}^-, \text{aq})$ were taken to be equal to the measured values of $V_2^0(\text{R}_3\text{NH}^+\text{Cl}^-, \text{aq})$ reported later in this paper. The values of $V_{\phi,2}(\text{Cl}^-, \text{aq}) \equiv V_2^0(\text{Cl}^-, \text{aq})$ and $V_{\phi,2}(\text{OH}^-, \text{aq}) \equiv V_2^0(\text{OH}^-, \text{aq})$ were taken from the database by Shock and Helgeson,²⁹ as calculated from their SUPCRT92 software.³⁰ The magnitude of the correction for these alkanol- and alkoxyamines was found to be less than 0.5

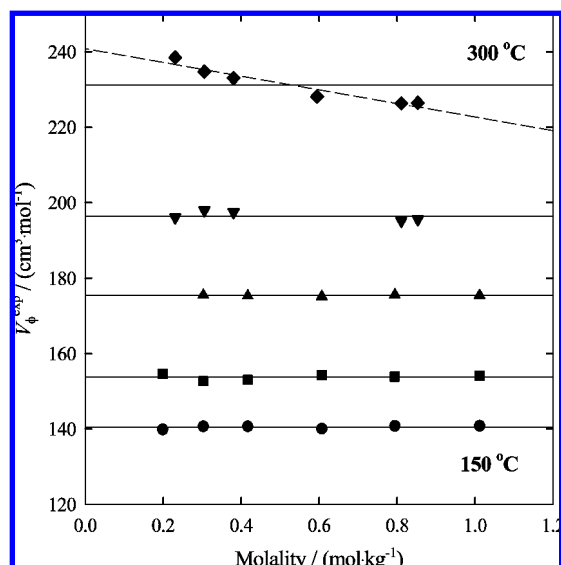


Figure 1. Apparent molar volumes, V_{ϕ}^{exp} , of aqueous 2-diethylethanolamine (2-DEEA) from 150 to 300 °C plotted as a function of molality. Symbols are experimental results, and lines represent the average value. ● at 150 °C, ■ at 200 °C, ▲ at 250 °C, ▼ at 275 °C, and ◆ at 300 °C. The molality-dependent fit at 300 °C is shown by the dashed line.

TABLE 6: Standard Partial Molar Volumes, V_2^0 , for Alkanolamines and Alkoxyamines Obtained Using Equation 5

t °C	p MPa	V_2^0 ($\text{cm}^3\cdot\text{mol}^{-1}$) ^a	t °C	p MPa	V_2^0 ($\text{cm}^3\cdot\text{mol}^{-1}$) ^a
ethylethanolamine (EAE)			2-diethylethanolamine (2-DEEA)		
150.87	15.24	104.04 ± 0.37	149.54	15.41	140.52 ± 0.42
200.72	15.25	112.37 ± 0.20	199.19	15.39	153.81 ± 0.76
250.32	15.24	124.26 ± 0.90	249.22	15.39	175.39 ± 0.18
275.23	15.26	135.08 ± 1.02	275.42	15.32	196.41 ± 1.20
300.18	15.25	153.67 ± 3.09	300.34	15.31	231.22 ± 4.98
		(159.34 ± 1.28) ^b			(240.82 ± 3.70) ^d
325.13	15.26	191.88 ± 2.18			
		(193.53 ± 2.07) ^b			
3-methoxypropylamine (3-MPA)			dimethylethanolamine (DMEA)		
149.23	15.29	108.12 ± 0.27	150.90	15.38	105.60 ± 0.06
200.78	15.24	117.17 ± 0.43	200.60	15.14	114.64 ± 0.11
246.51	15.31	128.59 ± 0.51	250.48	15.15	127.00 ± 0.03
275.29	15.26	140.36 ± 0.21	275.35	15.13	138.69 ± 0.05
299.97	15.30	155.28 ± 0.60	300.31	15.13	154.77 ± 0.69
325.41	15.31	204.27 ± 8.33	325.22	15.13	194.32 ± 0.81
		(217.41 ± 2.12) ^c			
340.26	16.95	267.61 ± 20.83			
		(307.15 ± 7.12) ^c			
monoethanolamine (MEA)			diethanolamine (DEA)		
150.30	15.17	64.67 ± 0.63	150.37	15.20	101.67 ± 0.08
200.36	15.18	67.98 ± 0.42	200.37	15.18	106.84 ± 0.35
250.11	15.19	72.63 ± 0.88	250.12	15.18	113.39 ± 0.22
300.24	15.17	82.60 ± 0.46	300.23	15.18	125.35 ± 0.28
325.13	15.18	106.68 ± 0.24	325.11	15.19	144.21 ± 1.15
triethanolamine (TEA)					
150.47	15.18	139.62 ± 0.03			
200.38	15.18	146.30 ± 0.05			
250.17	15.17	154.37 ± 0.24			
300.25	15.17	167.36 ± 1.30			
325.21	15.17	185.54 ± 1.57			

^a Error limits correspond to standard deviations; $B_V = 0$ unless otherwise noted. ^b B_V ($\text{cm}^3\cdot\text{kg}\cdot\text{mol}^{-2}$) = (-9.89 ± 0.82) at 300 °C and (-2.87 ± 3.23) at 325 °C. ^c B_V ($\text{cm}^3\cdot\text{kg}\cdot\text{mol}^{-2}$) = (-22.30 ± 3.15) at 325 °C and (-59.16 ± 9.69) at 340 °C. ^d B_V ($\text{cm}^3\cdot\text{kg}\cdot\text{mol}^{-2}$) = (-18.12 ± 2.59) at 300 °C.

$\text{cm}^3\cdot\text{mol}^{-1}$ at all the temperatures studied. The corrected values for $V_{\phi,2}$ are included in Tables 2–5, along with statistical uncertainties calculated from errors propagation expression given

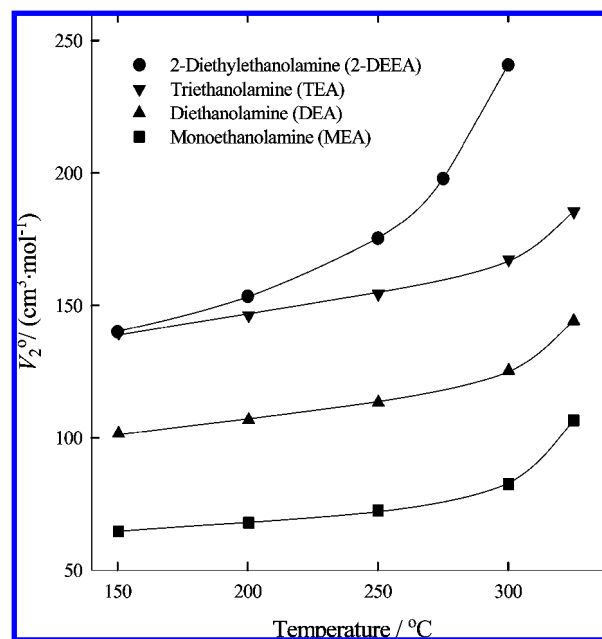


Figure 2. Standard partial molar volumes, V_2^0 , of monoethanolamine (MEA), diethanolamine (DEA), triethanolamine (TEA), and 2-diethylethanolamine (2-DEEA) plotted as a function of temperature. The lines represent global fit of eq 15, and symbols are experimental results.

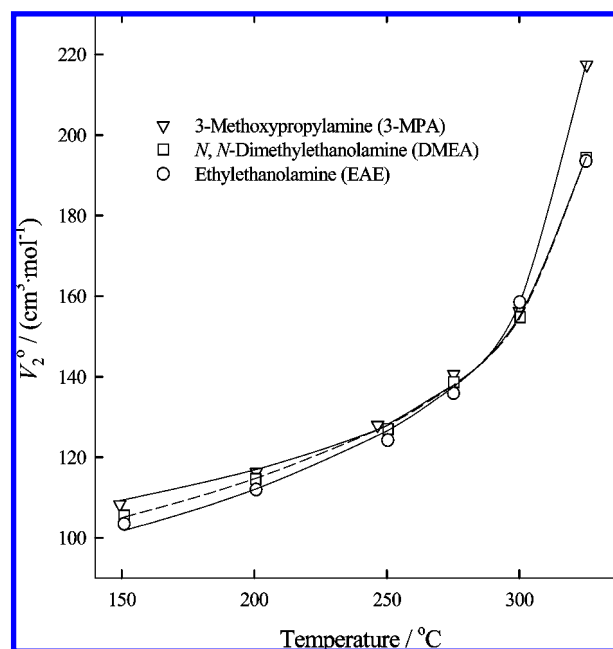


Figure 3. Standard partial molar volumes, V_2^0 , of the $\text{C}_4\text{H}_{11}\text{NO}$ isomers: N,N -dimethylethanolamine (DMEA), ethylethanolamine (EAE), and 3-methoxypropylamine (3-MPA) plotted as a function of temperature. The lines represent the global fit of eq 15, and symbols are experimental results.

in our previous work.²⁷ These include the standard deviations in the measured resonant frequencies of the densimeter, systematic errors in the molality, and other terms.

The standard partial molar volumes of EAE(aq), 2-DEEA(aq), and 3-MPA(aq) were determined by fitting linear equations to the molality dependent experimental results for $V_{\phi}(\text{R}_3\text{N}, \text{aq})$ and extrapolating to infinite dilution according to the expression

$$V_{\phi,2} = V_2^0 + B_V m \quad (5)$$

TABLE 7: Apparent Molar Volume $V_{\phi,2}$ for Aqueous (Ethylammonium)ethanol Chloride, Where Subscripts “2” and “3” Denote EAEH^+Cl^- and HCl , Respectively, $(\rho - \rho_1^*)$ is the Relative Density of Solution to Water, and $F_3 = m_3/(m_2 + m_3)$

t °C	p MPa	m_2 $\text{mol}\cdot\text{kg}^{-1}$	m_3 $\text{mol}\cdot\text{kg}^{-1}$	$10^2(\rho - \rho_1^*)$ $\text{g}\cdot\text{cm}^{-3}$	V_{ϕ}^{exp} $\text{cm}^3\cdot\text{mol}^{-1}$	$F_3V_{\phi,3}$ $\text{cm}^3\cdot\text{mol}^{-1}$	$V_{\phi,2}$ $\text{cm}^3\cdot\text{mol}^{-1}$
$t = (150.91 \pm 0.02)^\circ\text{C}; p = (15.24 \pm 0.01) \text{ MPa}; A_V = 6.98 \text{ cm}^3\cdot\text{kg}^{1/2}\cdot\text{mol}^{-3/2}$							
150.90	15.24	0.9313	0.1430	-2.0672	98.32	1.30	111.92 \pm 0.04
150.92	15.25	0.7969	0.1242	-1.8018	98.07	1.32	111.83 \pm 0.04
150.92	15.25	0.6285	0.0997	-1.4579	97.70	1.34	111.65 \pm 0.03
150.92	15.24	0.3949	0.0644	-0.9608	96.88	1.37	111.07 \pm 0.02
150.92	15.25	0.3219	0.0529	-0.7923	96.70	1.38	110.98 \pm 0.03
150.88	15.24	0.2008	0.0335	-0.5140	95.89	1.39	110.25 \pm 0.04
$t = (200.77 \pm 0.04)^\circ\text{C}; p = (15.25 \pm 0.01) \text{ MPa}; A_V = 13.43 \text{ cm}^3\cdot\text{kg}^{1/2}\cdot\text{mol}^{-3/2}$							
200.82	15.24	0.9313	0.1430	-2.5191	96.66	-0.22	116.13 \pm 0.05
200.76	15.26	0.7969	0.1242	-2.2091	96.14	-0.22	111.37 \pm 0.05
200.79	15.25	0.6285	0.0997	-1.8004	95.42	-0.22	110.82 \pm 0.03
200.80	15.25	0.3949	0.0644	-1.1958	94.06	-0.23	109.65 \pm 0.04
200.74	15.25	0.3219	0.0529	-0.9882	93.74	-0.23	109.41 \pm 0.03
200.71	15.24	0.2008	0.0335	-0.6395	92.74	-0.23	108.46 \pm 0.03
$t = (250.36 \pm 0.03)^\circ\text{C}; p = (15.25 \pm 0.01) \text{ MPa}; A_V = 29.33 \text{ cm}^3\cdot\text{kg}^{1/2}\cdot\text{mol}^{-3/2}$							
250.37	15.26	0.9313	0.1430	-3.2422	90.73	-3.16	108.31 \pm 0.09
250.38	15.25	0.7969	0.1242	-2.8563	89.75	-3.20	107.43 \pm 0.08
250.38	15.26	0.6285	0.0997	-2.3440	88.33	-3.25	106.11 \pm 0.06
250.34	15.24	0.3949	0.0644	-1.5811	85.47	-3.32	103.26 \pm 0.06
250.30	15.25	0.3219	0.0529	-1.3162	84.59	-3.35	102.38 \pm 0.07
250.37	15.25	0.2008	0.0335	-0.8514	83.05	-3.39	100.84 \pm 0.07
$t = (275.25 \pm 0.02)^\circ\text{C}; p = (15.25 \pm 0.01) \text{ MPa}; A_V = 47.43 \text{ cm}^3\cdot\text{kg}^{1/2}\cdot\text{mol}^{-3/2}$							
275.23	15.24	0.9313	0.1430	-3.7847	84.09	-5.78	103.66 \pm 0.07
275.22	15.26	0.7969	0.1242	-3.3400	82.70	-5.85	102.35 \pm 0.07
275.24	15.26	0.6285	0.0997	-2.7527	80.57	-5.95	100.25 \pm 0.07
275.26	15.25	0.3949	0.0644	-1.8553	76.89	-6.08	96.49 \pm 0.04
275.28	15.25	0.3219	0.0529	-1.5448	75.72	-6.13	95.29 \pm 0.06
275.28	15.25	0.2008	0.0335	-1.0112	72.83	-6.20	92.20 \pm 0.05
$t = (300.16 \pm 0.01)^\circ\text{C}; p = (15.25 \pm 0.01) \text{ MPa}; A_V = 85.78 \text{ cm}^3\cdot\text{kg}^{1/2}\cdot\text{mol}^{-3/2}$							
300.15	15.26	0.9313	0.1430	-4.5378	72.02	-10.30	94.95 \pm 0.08
300.16	15.25	0.7969	0.1242	-4.0332	69.51	-10.43	92.39 \pm 0.10
300.16	15.23	0.6285	0.0997	-3.3397	66.12	-10.59	88.89 \pm 0.06
300.17	15.25	0.3949	0.0644	-2.2762	59.89	-10.84	82.25 \pm 0.08
300.16	15.26	0.3219	0.0529	-1.9104	57.44	-10.92	79.59 \pm 0.05
300.18	15.25	0.2008	0.0335	-1.2714	51.59	-11.05	73.08 \pm 0.06
$t = (325.10 \pm 0.02)^\circ\text{C}; p = (15.26 \pm 0.01) \text{ MPa}; A_V = 196.05 \text{ cm}^3\cdot\text{kg}^{1/2}\cdot\text{mol}^{-3/2}$							
325.14	15.25	0.9313	0.1430	-5.9982	41.12	-20.64	71.24 \pm 0.24
325.11	15.25	0.7969	0.1242	-5.4136	35.10	-20.90	64.72 \pm 0.27
325.08	15.27	0.6285	0.0997	-4.4905	29.20	-21.23	58.44 \pm 0.12
325.09	15.26	0.3949	0.0644	-3.1552	14.20	-21.72	41.77 \pm 0.19
325.08	15.26	0.3219	0.0529	-2.6768	8.24	-21.88	35.07 \pm 0.21
325.11	15.26	0.2008	0.0335	-1.7774	-1.64	-22.14	23.92 \pm 0.15

The molality dependence is not large. Only at temperatures above 300 °C was the inclusion of the B_V term statistically significant. At temperatures below 300 °C, the extrapolated value of V_2^0 differed from the simple average of $V_{\phi,2}$ at all molalities by less than $1 \text{ cm}^3\cdot\text{mol}^{-1}$ when B_V was included. The values of V_2^0 and B_V for EAE(aq), 2-DEEA(aq) and 3-MPA(aq), as calculated after correction for the effects of ionization, are listed in Table 6 along with the value of V_2^0 obtained by taking a simple average. Although no decomposition products were detected by NMR at the highest temperatures reported, our experience suggests that decomposition usually results in more scatter in the measured apparent molar volumes for neutral species, with higher values at low molalities. The experimental values of $V_{\phi,2}$ for 2-DEEA(aq) at 300 °C and 3-MPA(aq) at 325 and 340 °C do show significant molality dependence. We therefore chose to use the simple average ($B_V = 0$) rather than the fitted values of V_2^0 from eq 5 in the group additivity treatment, presented below. However, the values of V_2^0 for 2-DEEA(aq) and 3-MPA(aq) at these temperatures using either method are suspect.

Standard partial molar volumes for the other alkanolamines were estimated by averaging the two $V_{\phi,2}$ values obtained at $m \approx 0.5 \text{ mol}\cdot\text{kg}^{-1}$, as listed in Table 5, for each experimental temperature and pressure. This approach is similar to that of Criss and Wood⁸ and Schulte et al.³¹ in assuming that $V_{\phi,2}$ for neutral species is not dependent on molality. The resulting standard partial molar volumes, V_2^0 , for aqueous MEA(aq), DEA(aq), TEA(aq) and DMEA(aq) are also tabulated in Table 6.

The standard partial molar volumes for all the neutral species studied in this work, are plotted in Figures 2 and 3. The increasing values of V_2^0 with temperature are consistent with the behavior of most nonelectrolytes in which hydrophobic effects are enhanced by the sharply increasingly isothermal compressibility of water as it approaches the critical point.^{14,15,32} The values of V_2^0 for the species in Figure 2, show a progressive increase in the order $\text{MEA} < \text{DEA} < \text{TEA}$ as the structure is changed from primary to secondary to tertiary amine by replacing hydrogen with ethanolic groups on the central nitrogen atom. 2-DEEA is similar in size to TEA, and the much

TABLE 8: Apparent Molar Volume $V_{\phi,2}$ for Aqueous 2-Diethylethanolammonium Chloride, Where Subscripts “2” and “3” Denote 2-DEEAH⁺Cl[−] and HCl, Respectively, $(\rho - \rho_1^*)$ is the Relative Density of Solution to Water, and $F_3 = m_3/(m_2 + m_3)$

t °C	p MPa	m_2 mol·kg ^{−1}	m_3 mol·kg ^{−1}	$10^2 \cdot (\rho - \rho_1^*)$ g·cm ^{−3}	V_{ϕ}^{exp} cm ³ ·mol ^{−1}	$F_3 V_{\phi,3}$ cm ³ ·mol ^{−1}	$V_{\phi,2}$ cm ³ ·mol ^{−1}
$t = (149.16 \pm 0.02)^\circ\text{C}; p = (15.40 \pm 0.02) \text{ MPa}; A_V = 6.83 \text{ cm}^3 \cdot \text{kg}^{1/2} \cdot \text{mol}^{-3/2}$							
149.18	15.41	0.7735	0.0000	−1.1515	146.74	0.00	146.74 ± 0.05
149.17	15.39	0.5942	0.0000	−0.9076	146.68	0.00	146.68 ± 0.05
149.17	15.38	0.4064	0.0185	−0.7050	139.99	0.43	145.93 ± 0.05
149.14	15.39	0.2921	0.0136	−0.5227	139.58	0.43	145.60 ± 0.05
149.15	15.39	0.2048	0.0096	−0.3766	139.20	0.44	145.28 ± 0.05
149.13	15.42	0.1596	0.0076	−0.3070	138.33	0.44	144.42 ± 0.05
$t = (200.74 \pm 0.04)^\circ\text{C}; p = (15.38 \pm 0.02) \text{ MPa}; A_V = 13.41 \text{ cm}^3 \cdot \text{kg}^{1/2} \cdot \text{mol}^{-3/2}$							
200.76	15.38	0.7735	0.0000	−1.4510	148.78	0.00	148.78 ± 0.08
200.70	15.36	0.5942	0.0000	−1.1501	148.50	0.00	148.50 ± 0.09
200.76	15.39	0.4064	0.0185	−0.9288	139.85	−0.07	146.31 ± 0.07
200.69	15.39	0.2921	0.0136	−0.6714	140.01	−0.07	146.59 ± 0.08
200.76	15.40	0.2048	0.0096	−0.4825	139.56	−0.07	146.19 ± 0.08
$t = (249.21 \pm 0.09)^\circ\text{C}; p = (15.41 \pm 0.01) \text{ MPa}; A_V = 28.68 \text{ cm}^3 \cdot \text{kg}^{1/2} \cdot \text{mol}^{-3/2}$							
249.05	15.43	0.7735	0.0000	−1.9211	147.93	0.00	147.93 ± 0.10
249.24	15.41	0.5942	0.0000	−1.5511	146.74	0.00	146.74 ± 0.09
249.30	15.40	0.4064	0.0185	−1.2262	137.03	−1.03	144.36 ± 0.09
249.24	15.42	0.2921	0.0136	−0.9267	135.23	−1.05	142.60 ± 0.11
249.23	15.41	0.2048	0.0096	−0.6633	134.66	−1.06	142.11 ± 0.09
249.23	15.40	0.1596	0.0076	−0.5450	132.31	−1.07	139.69 ± 0.10
$t = (275.50 \pm 0.05)^\circ\text{C}; p = (15.33 \pm 0.01) \text{ MPa}; A_V = 47.61 \text{ cm}^3 \cdot \text{kg}^{1/2} \cdot \text{mol}^{-3/2}$							
275.52	15.32	0.8678	0.2437	−3.4538	108.75	−9.52	151.49 ± 0.08
275.56	15.34	0.5525	0.1616	−2.3976	105.09	−9.83	148.54 ± 0.09
275.54	15.34	0.4035	0.1204	−1.8510	102.42	−9.98	145.94 ± 0.06
275.47	15.31	0.3060	0.0925	−1.4499	100.86	−10.08	144.48 ± 0.05
275.46	15.32	0.2089	0.0640	−1.0537	97.31	−10.18	140.44 ± 0.06
275.42	15.32	0.1567	0.0484	−0.8104	95.91	−10.24	138.91 ± 0.05
$t = (300.40 \pm 0.05)^\circ\text{C}; p = (15.32 \pm 0.01) \text{ MPa}; A_V = 86.17 \text{ cm}^3 \cdot \text{kg}^{1/2} \cdot \text{mol}^{-3/2}$							
300.43	15.32	0.8678	0.2437	−4.1172	100.30	−16.96	150.20 ± 0.09
300.44	15.32	0.5525	0.1616	−2.9323	93.45	−17.51	143.41 ± 0.12
300.45	15.32	0.4035	0.1204	−2.2648	89.74	−17.78	139.60 ± 0.07
300.41	15.31	0.3060	0.0925	−1.7853	87.04	−17.96	136.75 ± 0.10
300.34	15.32	0.2089	0.0640	−1.2864	82.87	−18.14	131.97 ± 0.06
300.34	15.31	0.1567	0.0484	−1.0033	79.63	−18.24	128.08 ± 0.07

sharper rise in V_2° (2-DEEA) with increasing temperature is consistent with the more hydrophobic nature of the two ethyl side chains.

Figure 3 shows the temperature dependence of V_2° for three isomers with the formula $\text{C}_4\text{H}_{11}\text{NO}$. EAE and DMEA are secondary and tertiary monoethanolamines, and 3-MPA is an alkoxyamine. The values of V_2° agree to within $5 \text{ cm}^3 \cdot \text{mol}^{-1}$ over most of the temperature range, reflecting the very similar intrinsic molar volumes of these three molecules. The more positive value for 3-MPA ($+23 \text{ cm}^3 \cdot \text{mol}^{-1}$) observed above 300°C is consistent with the hydrophobicity of its ether group relative to the hydroxy group on each of the two ethanolamines, although the effect is also consistent with thermal decomposition.

Experimental values of the apparent molar volumes, V_{ϕ}^{exp} , of the chloride salts are listed in Tables 7 to 10. As in our earlier work,^{11–13} the effect of the excess HCl was subtracted by applying Young's rule as follows

$$V_{\phi,2}(\text{R}_3\text{NH}^+\text{Cl}^-, \text{aq}) = \{V_{\phi}^{\text{exp}}(m_2 + m_3) - V_{\phi,3}(\text{H}^+\text{Cl}^-, \text{aq})m_3\}/m_2 \quad (6)$$

where m_2 , $V_{\phi,2}$, m_3 , and $V_{\phi,3}$ are the molality and the contribution to V_{ϕ}^{exp} of the alkanolammonium chloride and the excess HCl, respectively. In these very dilute solutions, $V_{\phi,3}(\text{H}^+\text{Cl}^-, \text{aq})$ were assumed to be approximately equal to $V_3^\circ(\text{H}^+\text{Cl}^-, \text{aq})$ whose values were obtained from Sharygin and Wood.³³ The variation of $V_{\phi,2}$ with ionic strength at each temperature was

obtained from least-squares fits of a simple Debye–Hückel equation

$$V_{\phi,2} = V_2^\circ + A_V I^{1/2} + B_V I \quad (7)$$

where V_2° is the partial molar volume at infinite dilution, I is the ionic strength and B_V is an adjustable parameter which accounts for solute–solute interactions. The Debye–Hückel coefficient for volume, A_V , was obtained from the formulation reported by Archer and Wang.³⁴ The values of V_2° for the chloride salts of the 3-MPA, EAE, 2-DEEA, DMEA, MEA, DEA, and TEA thus obtained are tabulated in Table 11, along with the fitted values of B_V and the standard deviations in both parameters. We note that with the exception of TEAH⁺Cl[−] the values of B_V at each temperature are in very close agreement despite the fact that the solute molecules contain primary, secondary, and tertiary amine groups, respectively. Values for one of these chloride salts, $V_{\phi,2}$ (2-DEEAH⁺Cl[−]), are plotted in Figure 4 as a typical example of a least-squares fit of eq 7 to the data for these species. Our initial measurements on DMEA, MEA, DEA, and TEA were carried on only two solutions, $m \approx 0.5 \text{ mol kg}^{-1}$, in the expectation that V_2° could be calculated from eq 7 using only the theoretical A_V term, as was done by Criss and Wood⁸ at lower temperatures. When it became apparent that more data points were needed for an accurate extrapolation, a second set of solutions were prepared from new stock solutions. Both sets of values are listed in the table, and both were used in the least-squares fits. The standard deviations

TABLE 9: Apparent Molar Volume $V_{\phi,2}$ for Aqueous 3-Methoxypropylammonium Chloride, Where Subscripts “2” and “3” Denote 3-MPAH⁺Cl[−] and HCl, Respectively, $(\rho - \rho_1^*)$ is the Relative Density of Solution to Water, and $F_3 = m_3/(m_2 + m_3)$

t °C	p MPa	m_2 mol·kg ^{−1}	m_3 mol·kg ^{−1}	$10^2 \cdot (\rho - \rho_1^*)$ g·cm ^{−3}	V_{ϕ}^{exp} cm ³ ·mol ^{−1}	$F_3 V_{\phi,3}$ cm ³ ·mol ^{−1}	$V_{\phi,2}$ cm ³ ·mol ^{−1}
$t = (149.30 \pm 0.03) \text{ }^\circ\text{C}; p = (15.30 \pm 0.01) \text{ MPa}; A_V = 6.84 \text{ cm}^3 \cdot \text{kg}^{1/2} \cdot \text{mol}^{-3/2}$							
149.34	15.32	1.0133	0.0757	−1.7727	107.91	0.68	115.25 ± 0.09
149.33	15.31	0.7945	0.0608	−1.4552	107.28	0.69	114.75 ± 0.07
149.33	15.31	0.5933	0.0465	−1.1252	106.85	0.71	114.45 ± 0.08
149.28	15.30	0.4143	0.0331	−0.8279	106.00	0.72	113.69 ± 0.14
149.27	15.29	0.3059	0.0248	−0.6577	104.50	0.73	112.17 ± 0.12
149.28	15.30	0.2087	0.0171	−0.4326	105.53	0.74	113.38 ± 0.10
$t = (200.75 \pm 0.04) \text{ }^\circ\text{C}; p = (15.25 \pm 0.01) \text{ MPa}; A_V = 13.43 \text{ cm}^3 \cdot \text{kg}^{1/2} \cdot \text{mol}^{-3/2}$							
200.75	15.24	0.9256	0.1410	−2.2106	100.55	−0.22	116.13 ± 0.04
200.80	15.31	0.7843	0.1213	−1.9119	100.22	−0.22	115.98 ± 0.06
200.79	15.26	0.5828	0.0922	−1.4958	99.08	−0.22	115.01 ± 0.03
200.71	15.25	0.3728	0.0604	−0.9894	98.48	−0.23	114.70 ± 0.03
200.72	15.23	0.2949	0.0482	−0.8023	97.88	−0.23	114.14 ± 0.03
200.74	15.24	0.2160	0.0356	−0.6159	96.55	−0.23	112.75 ± 0.02
$t = (246.47 \pm 0.04) \text{ }^\circ\text{C}; p = (15.30 \pm 0.01) \text{ MPa}; A_V = 27.37 \text{ cm}^3 \cdot \text{kg}^{1/2} \cdot \text{mol}^{-3/2}$							
246.43	15.31	1.0133	0.0757	−2.8591	103.24	−1.65	112.72 ± 0.15
246.49	15.30	0.7945	0.0608	−2.3471	101.97	−1.69	111.59 ± 0.17
246.47	15.31	0.5933	0.0465	−1.8338	100.64	−1.72	110.38 ± 0.14
246.43	15.30	0.4143	0.0331	−1.3656	98.32	−1.75	108.07 ± 0.13
246.49	15.30	0.3059	0.0248	−1.0367	97.38	−1.78	107.18 ± 0.11
246.52	15.31	0.2087	0.0171	−0.7332	96.01	−1.79	105.82 ± 0.13
$t = (275.36 \pm 0.06) \text{ }^\circ\text{C}; p = (15.33 \pm 0.01) \text{ MPa}; A_V = 47.47 \text{ cm}^3 \cdot \text{kg}^{1/2} \cdot \text{mol}^{-3/2}$							
275.36	15.33	1.0133	0.0757	−3.4035	97.90	−3.02	108.46 ± 0.10
275.37	15.33	0.7945	0.0608	−2.8194	95.67	−3.09	106.32 ± 0.06
275.46	15.33	0.5933	0.0465	−2.2193	93.42	−3.15	104.13 ± 0.06
275.30	15.33	0.4143	0.0331	−1.6406	90.68	−3.21	101.40 ± 0.06
275.32	15.33	0.3059	0.0248	−1.2541	88.95	−3.25	99.66 ± 0.05
275.37	15.33	0.2087	0.0171	−0.9043	85.76	−3.29	96.34 ± 0.04
$t = (299.98 \pm 0.04) \text{ }^\circ\text{C}; p = (15.31 \pm 0.01) \text{ MPa}; A_V = 85.21 \text{ cm}^3 \cdot \text{kg}^{1/2} \cdot \text{mol}^{-3/2}$							
300.00	15.32	1.0133	0.0757	−4.1907	86.46	−5.38	98.70 ± 0.16
299.94	15.30	0.7945	0.0608	−3.4685	83.35	−5.50	95.65 ± 0.09
300.00	15.30	0.5933	0.0465	−2.7562	79.34	−5.62	91.61 ± 0.12
300.02	15.31	0.4143	0.0331	−2.0491	74.91	−5.73	87.08 ± 0.09
300.00	15.32	0.3059	0.0248	−1.5889	71.08	−5.79	83.09 ± 0.09
299.93	15.32	0.2087	0.0171	−1.1548	65.67	−5.86	77.39 ± 0.11
$t = (325.43 \pm 0.04) \text{ }^\circ\text{C}; p = (15.32 \pm 0.01) \text{ MPa}; A_V = 197.96 \text{ cm}^3 \cdot \text{kg}^{1/2} \cdot \text{mol}^{-3/2}$							
325.45	15.34	1.0133	0.0757	−5.6045	58.25	−10.78	74.19 ± 0.24
325.47	15.33	0.7945	0.0608	−4.7870	49.21	−11.02	64.84 ± 0.14
325.47	15.32	0.5933	0.0465	−3.8278	41.41	−11.26	56.79 ± 0.22
325.44	15.32	0.4143	0.0331	−2.9117	30.42	−11.48	45.24 ± 0.24
325.36	15.31	0.3059	0.0248	−2.2850	21.79	−11.61	36.10 ± 0.18
325.39	15.32	0.2087	0.0171	−1.6316	14.96	−11.74	28.88 ± 0.18
$t = (340.25 \pm 0.04) \text{ }^\circ\text{C}; p = (16.94 \pm 0.01) \text{ MPa}; A_V = 367.23 \text{ cm}^3 \cdot \text{kg}^{1/2} \cdot \text{mol}^{-3/2}$							
340.22	16.95	1.0133	0.0757	−6.0737	43.69	−16.94	65.16 ± 0.51
340.23	16.94	0.7945	0.0608	−5.6534	19.34	−17.32	39.47 ± 0.25
340.28	16.94	0.5933	0.0465	−4.8334	−3.30	−17.69	15.52 ± 0.15
340.28	16.94	0.4143	0.0331	−3.7282	−22.48	−18.03	−4.80 ± 0.35
340.28	16.94	0.3059	0.0248	−2.9292	−35.86	−18.25	−19.03 ± 0.16
340.19	16.94	0.2087	0.0171	−2.1036	−47.61	−18.44	−31.56 ± 0.34

of the fitted values V_2° were taken as our estimates of uncertainty. These are approximately equal to the 95% confidence limits.

The standard partial molar volumes for all the chloride salts are plotted as a function of temperature in Figures 5 and 6. The experimental values of V_2° for all the chloride salts show the expected deviation toward very large negative values with increasing temperature, consistent with both the Born equation³⁵ and a negative Krichevskii parameter.^{14,15,32} This behavior is true of all known electrolytes. The contribution of the chloride ion is the largest effect.^{11,12}

3.2. Comparison with Other Studies. There have been many investigations over the years on thermodynamic properties of aqueous solutions of amines, most of which are limited to near-ambient conditions. Density values of alkanolamines up to 160 °C obtained by DiGuillo et al.³⁶ are among the very few

studies above 100 °C. Cabani and co-workers³⁷ published ΔV_2° and $\Delta C_{p,2}^\circ$ values for proton addition to 3-MPA, MEA, EAE, 2-DEEA and other amines in the temperature range 25 °C ≤ t ≤ 40 °C. Densities, excess molar volumes, and partial molar volume for binary mixtures of water with MEA, DEA, TEA, and DMEA at temperature up to 80 °C were published by Maham and co-workers.^{38–40} Recently, Hawrylak et al.⁴¹ published partial molar and excess volumes and adiabatic compressibility of binary mixtures of alkanolamines with water at 25–45 °C. Thermodynamic properties of aqueous DEA and DMEA were obtained by Collins et al.⁴² at temperatures up to 55 °C. Densities and excess molar volumes of DMEA and 2-DEEA in water from 20 to 40 °C were also reported by Zhang et al.⁴³ Other studies reporting the volumetric properties of EAE and 2-DEEA include that of Lebrette et al.⁴⁴ to temperatures up to 80 °C and measurements by Lampreia et al.⁴⁵ and Barbas

TABLE 10: Apparent Molar Volume $V_{\phi,2}$ for Other Aqueous Chlorides, Where $(\rho - \rho_1^*)$ is the Relative Density of Solution to Water, and $F_3 = m_3/(m_2 + m_3)$

t °C	p MPa	m_2 mol·kg ⁻¹	m_3 mol·kg ⁻¹	$10^2 \cdot (\rho - \rho_1^*)$ g·cm ⁻³	V_{ϕ}^{exp} cm ³ ·mol ⁻¹	$F_3 V_{\phi,3}$ cm ³ ·mol ⁻¹	$V_{\phi,2}$ cm ³ ·mol ⁻¹
a: monoethanolammonium chlorides, where subscripts “2” and “3” denote MEAH ⁺ Cl ⁻ and HCl, respectively							
$t = (150.35 \pm 0.09)^\circ\text{C}; p = (15.15 \pm 0.04) \text{ MPa}; A_V = 6.94 \text{ cm}^3 \cdot \text{kg}^{1/2} \cdot \text{mol}^{-3/2}$							
150.29	15.12	0.9217	0.0297	-2.5255	70.45	0.30	72.41 ± 0.06
150.29	15.12	0.5967	0.0198	-1.7122	69.58	0.31	71.57 ± 0.05
150.47	15.17	0.4811	0.0410	-1.4744	66.22	0.76	71.03 ± 0.02
150.47	15.17	0.4839	0.0412	-1.4825	66.22	0.76	71.03 ± 0.03
150.29	15.13	0.2991	0.0102	-0.9115	68.16	0.32	70.15 ± 0.06
150.29	15.21	0.1885	6.5038e-3	-0.5859	67.69	0.32	69.69 ± 0.07
$t = (200.17 \pm 0.13)^\circ\text{C}; p = (15.12 \pm 0.05) \text{ MPa}; A_V = 13.34 \text{ cm}^3 \cdot \text{kg}^{1/2} \cdot \text{mol}^{-3/2}$							
200.05	15.08	0.5967	0.0198	-2.0757	63.75	-0.05	65.92 ± 0.08
200.32	15.17	0.4811	0.0410	-1.7452	61.13	-0.13	66.49 ± 0.03
200.30	15.18	0.4839	0.0412	-1.7627	60.93	-0.13	66.27 ± 0.03
200.09	15.07	0.2991	0.0102	-1.2017	57.63	-0.05	59.66 ± 0.10
200.11	15.08	0.1885	6.5038e-3	-0.7773	56.57	-0.06	58.58 ± 0.08
$t = (250.14 \pm 0.05)^\circ\text{C}; p = (15.11 \pm 0.04) \text{ MPa}; A_V = 29.28 \text{ cm}^3 \cdot \text{kg}^{1/2} \cdot \text{mol}^{-3/2}$							
250.20	15.08	0.5967	0.0198	-2.5825	52.49	-0.77	55.02 ± 0.10
250.17	15.15	0.4811	0.0410	-2.2183	48.44	-1.86	54.59 ± 0.08
250.15	15.16	0.4839	0.0412	-2.2331	48.37	-1.86	54.51 ± 0.08
250.10	15.08	0.2991	0.0102	-1.4226	47.03	-0.78	49.45 ± 0.10
250.08	15.08	0.1885	6.5038e-3	-0.9593	42.45	-0.79	44.73 ± 0.09
$t = (300.14 \pm 0.06)^\circ\text{C}; p = (15.11 \pm 0.05) \text{ MPa}; A_V = 86.10 \text{ cm}^3 \cdot \text{kg}^{1/2} \cdot \text{mol}^{-3/2}$							
300.14	15.07	0.9217	0.0297	-5.1659	26.76	-2.42	30.12 ± 0.10
300.09	15.08	0.5967	0.0198	-3.6024	19.76	-2.49	22.98 ± 0.08
300.21	15.17	0.4811	0.0410	-3.0894	14.80	-6.07	22.65 ± 0.05
300.22	15.17	0.4839	0.0412	-3.1032	14.93	-6.07	22.79 ± 0.08
300.09	15.08	0.2991	0.0102	-2.0049	8.30	-2.55	11.23 ± 0.08
300.08	15.08	0.1885	6.5038e-3	-1.3608	-0.93	-2.58	1.71 ± 0.08
$t = (325.14 \pm 0.06)^\circ\text{C}; p = (15.11 \pm 0.05) \text{ MPa}; A_V = 198.25 \text{ cm}^3 \cdot \text{kg}^{1/2} \cdot \text{mol}^{-3/2}$							
325.06	15.07	0.9217	0.0297	-6.8037	-16.22	-4.84	-11.76 ± 0.08
325.10	15.08	0.5967	0.0198	-4.8174	-30.77	-4.98	-26.65 ± 0.07
325.22	15.18	0.4811	0.0410	-4.1166	-36.57	-12.14	-26.52 ± 0.15
325.20	15.17	0.4839	0.0412	-4.1337	-36.30	-12.13	-26.23 ± 0.12
325.13	15.08	0.2991	0.0102	-2.7162	-52.84	-5.12	-49.35 ± 0.06
325.14	15.08	0.1885	6.5038e-3	-1.8056	-64.14	-5.17	-61.00 ± 0.06
b: diethanolammonium Chlorides, where subscripts “2” and “3” denote DEAH ⁺ Cl ⁻ and HCl, respectively							
$t = (150.36 \pm 0.10)^\circ\text{C}; p = (15.10 \pm 0.08) \text{ MPa}; A_V = 6.94 \text{ cm}^3 \cdot \text{kg}^{1/2} \cdot \text{mol}^{-3/2}$							
150.29	15.05	0.5915	0.0579	-2.1953	101.05	0.87	109.99 ± 0.09
150.47	15.18	0.4898	0.0508	-1.8728	99.91	0.91	109.26 ± 0.04
150.47	15.18	0.4874	0.0505	-1.8708	99.76	0.91	109.10 ± 0.05
150.28	15.04	0.2944	0.0299	-1.1526	99.82	0.90	108.98 ± 0.07
150.28	15.04	0.1972	0.0203	-0.8271	97.17	0.91	106.18 ± 0.08
$t = (200.17 \pm 0.14)^\circ\text{C}; p = (15.12 \pm 0.06) \text{ MPa}; A_V = 13.33 \text{ cm}^3 \cdot \text{kg}^{1/2} \cdot \text{mol}^{-3/2}$							
200.09	15.08	0.5915	0.0579	-2.5156	97.74	-0.15	107.47 ± 0.11
200.31	15.18	0.4898	0.0508	-2.1616	95.97	-0.16	106.10 ± 0.07
200.33	15.18	0.4874	0.0505	-2.1578	95.82	-0.16	105.93 ± 0.06
200.03	15.08	0.2944	0.0299	-1.3478	95.01	-0.15	104.84 ± 0.10
200.07	15.08	0.1972	0.0203	-0.9989	89.63	-0.15	99.03 ± 0.17
$t = (250.18 \pm 0.04)^\circ\text{C}; p = (15.11 \pm 0.06) \text{ MPa}; A_V = 29.30 \text{ cm}^3 \cdot \text{kg}^{1/2} \cdot \text{mol}^{-3/2}$							
250.23	15.07	0.5915	0.0579	-3.0645	87.98	-2.12	98.92 ± 0.14
250.17	15.17	0.4898	0.0508	-2.6343	85.55	-2.23	96.87 ± 0.13
250.14	15.18	0.4874	0.0505	-2.6139	85.78	-2.23	97.13 ± 0.14
250.15	15.08	0.2944	0.0299	-1.6340	84.32	-2.19	95.32 ± 0.11
250.22	15.07	0.1972	0.0203	-1.1452	81.31	-2.22	92.14 ± 0.13
$t = (300.12 \pm 0.02)^\circ\text{C}; p = (15.10 \pm 0.05) \text{ MPa}; A_V = 86.07 \text{ cm}^3 \cdot \text{kg}^{1/2} \cdot \text{mol}^{-3/2}$							
300.14	15.07	0.8916	0.0840	-5.6847	66.76	-6.67	80.35 ± 0.15
300.11	15.07	0.5915	0.0579	-4.0753	59.69	-6.90	73.10 ± 0.13
300.15	15.17	0.4898	0.0508	-3.4855	56.37	-7.25	70.21 ± 0.10
300.13	15.16	0.4874	0.0505	-3.4779	56.07	-7.25	69.88 ± 0.09
300.08	15.07	0.2944	0.0299	-2.2486	48.57	-7.14	61.38 ± 0.09
300.11	15.07	0.1972	0.0203	-1.4516	53.80	-7.23	67.32 ± 1.03
$t = (325.09 \pm 0.06)^\circ\text{C}; p = (15.11 \pm 0.06) \text{ MPa}; A_V = 197.60 \text{ cm}^3 \cdot \text{kg}^{1/2} \cdot \text{mol}^{-3/2}$							
325.01	15.08	0.8916	0.0840	-7.0810	31.84	-13.29	49.39 ± 0.11
325.05	15.08	0.5915	0.0579	-5.1846	17.01	-13.78	33.80 ± 0.12
325.12	15.19	0.4898	0.0508	-4.4324	11.93	-14.46	29.12 ± 0.16
325.16	15.19	0.4874	0.0505	-4.3944	12.57	-14.48	29.85 ± 0.23
325.12	15.07	0.2944	0.0299	-2.9365	-6.19	-14.31	8.94 ± 0.10
325.07	15.07	0.1972	0.0203	-2.0761	-17.10	-14.46	-2.91 ± 0.10

TABLE 10 (Continued)

t °C	p MPa	m_2 mol·kg ⁻¹	m_3 mol·kg ⁻¹	$10^2 \cdot (\rho - \rho_1^*)$ g·cm ⁻³	V_ϕ^{exp} cm ³ ·mol ⁻¹	$F_3 V_{\phi,3}$ cm ³ ·mol ⁻¹	$V_{\phi,2}$ cm ³ ·mol ⁻¹
c: triethanolammonium chlorides, where subscripts "2" and "3" denote TEAH ⁺ Cl ⁻ and HCl							
$t = (150.34 \pm 0.08)^\circ\text{C}; p = (15.08 \pm 0.08) \text{ MPa}; A_V = 6.94 \text{ cm}^3 \cdot \text{kg}^{1/2} \cdot \text{mol}^{-3/2}$							
150.29	15.04	0.5950	0.1450	-2.8123	121.02	1.90	148.14 ± 0.15
150.44	15.17	0.4802	0.1709	-2.4684	111.12	2.54	147.21 ± 0.05
150.41	15.18	0.4518	0.1615	-2.3321	111.01	2.55	147.22 ± 0.06
150.28	15.02	0.2957	0.0757	-1.4881	119.10	1.98	147.09 ± 0.10
150.28	15.01	0.1875	0.0489	-0.9684	118.26	2.01	146.55 ± 0.11
$t = (200.22 \pm 0.13)^\circ\text{C}; p = (15.12 \pm 0.06) \text{ MPa}; A_V = 13.34 \text{ cm}^3 \cdot \text{kg}^{1/2} \cdot \text{mol}^{-3/2}$							
200.13	15.07	0.5950	0.1450	-3.2187	117.66	-0.33	146.74 ± 0.17
200.36	15.20	0.4802	0.1709	-2.8091	107.66	-0.45	146.58 ± 0.07
200.35	15.18	0.4518	0.1615	-2.6764	107.04	-0.45	145.92 ± 0.08
200.13	15.07	0.2957	0.0757	-1.7195	114.73	-0.34	144.51 ± 0.13
200.11	15.07	0.1875	0.0489	-1.1260	113.29	-0.34	143.24 ± 0.11
$t = (250.11 \pm 0.08)^\circ\text{C}; p = (15.12 \pm 0.06) \text{ MPa}; A_V = 29.25 \text{ cm}^3 \cdot \text{kg}^{1/2} \cdot \text{mol}^{-3/2}$							
250.16	15.08	0.5950	0.1450	-3.8403	108.81	-4.66	141.12 ± 0.21
249.98	15.17	0.4802	0.1709	-3.3244	98.94	-6.20	142.55 ± 0.23
250.08	15.19	0.4518	0.1615	-3.1553	98.42	-6.23	142.06 ± 0.19
250.11	15.08	0.2957	0.0757	-2.0783	103.68	-4.84	136.28 ± 0.16
250.20	15.07	0.1875	0.0489	-1.3571	101.90	-4.92	134.65 ± 0.17
$t = (300.11 \pm 0.02)^\circ\text{C}; p = (15.07 \pm 0.01) \text{ MPa}; A_V = 85.95 \text{ cm}^3 \cdot \text{kg}^{1/2} \cdot \text{mol}^{-3/2}$							
300.13	15.07	0.7376	0.1757	-5.2263	100.37	-14.90	142.74 ± 0.18
300.11	15.06	0.5950	0.1450	-4.4365	95.84	-15.16	138.05 ± 0.17
300.10	15.06	0.2957	0.0757	-2.5398	81.21	-15.77	121.80 ± 0.12
300.11	15.07	0.1875	0.0489	-1.7342	72.29	-15.99	111.28 ± 0.11
$t = (325.06 \pm 0.07)^\circ\text{C}; p = (15.11 \pm 0.06) \text{ MPa}; A_V = 197.43 \text{ cm}^3 \cdot \text{kg}^{1/2} \cdot \text{mol}^{-3/2}$							
325.03	15.07	0.7376	0.1757	-6.1632	76.34	-29.74	131.36 ± 0.16
325.01	15.06	0.5950	0.1450	-5.2304	69.91	-30.28	124.60 ± 0.14
325.18	15.19	0.4802	0.1709	-4.4781	60.69	-40.48	137.18 ± 0.24
325.13	15.19	0.4518	0.1615	-4.2549	59.45	-40.55	135.75 ± 0.21
325.02	15.08	0.2957	0.0757	-2.9797	49.81	-31.46	102.07 ± 0.14
325.01	15.07	0.1875	0.0489	-2.0797	32.88	-31.91	81.67 ± 0.13
d: dimethylethanolammonium chlorides, where subscripts "2" and "3" denote DMEAH ⁺ Cl ⁻ and HCl, respectively							
$t = (150.43 \pm 0.27)^\circ\text{C}; p = (15.15 \pm 0.02) \text{ MPa}; A_V = 6.94 \text{ cm}^3 \cdot \text{kg}^{1/2} \cdot \text{mol}^{-3/2}$							
150.23	15.15	0.5991	0.0986	-1.3150	98.74	1.38	113.39 ± 0.08
150.75	15.13	0.4973	0.0670	-1.1359	99.64	1.14	111.76 ± 0.03
150.70	15.14	0.5028	0.0677	-1.1447	99.70	1.15	111.83 ± 0.04
150.22	15.17	0.2968	0.0506	-0.7079	97.20	1.42	112.10 ± 0.09
150.23	15.17	0.1954	0.0337	-0.4274	99.35	1.43	114.80 ± 0.06
$t = (200.35 \pm 0.29)^\circ\text{C}; p = (15.10 \pm 0.03) \text{ MPa}; A_V = 13.36 \text{ cm}^3 \cdot \text{kg}^{1/2} \cdot \text{mol}^{-3/2}$							
200.08	15.07	0.5991	0.0986	-1.7162	95.19	-0.23	111.13 ± 0.11
200.60	15.14	0.4973	0.0670	-1.4197	97.09	-0.21	110.41 ± 0.04
200.72	15.14	0.5028	0.0677	-1.4313	97.18	-0.22	110.51 ± 0.03
200.17	15.08	0.2968	0.0506	-0.8921	94.25	-0.24	110.59 ± 0.07
200.16	15.08	0.1954	0.0337	-0.5857	94.57	-0.25	111.16 ± 0.06
$t = (250.29 \pm 0.15)^\circ\text{C}; p = (15.11 \pm 0.03) \text{ MPa}; A_V = 29.35 \text{ cm}^3 \cdot \text{kg}^{1/2} \cdot \text{mol}^{-3/2}$							
250.13	15.09	0.5991	0.0986	-2.2220	88.49	-3.36	106.97 ± 0.13
250.44	15.13	0.4973	0.0670	-1.8964	88.67	-2.84	103.84 ± 0.09
250.46	15.15	0.5028	0.0677	-1.9197	88.58	-2.84	103.73 ± 0.08
250.19	15.08	0.2968	0.0506	-1.1898	85.54	-3.46	104.16 ± 0.10
250.22	15.08	0.1954	0.0337	-0.8303	82.75	-3.50	101.11 ± 0.10
$t = (300.17 \pm 0.09)^\circ\text{C}; p = (15.09 \pm 0.04) \text{ MPa}; A_V = 86.20 \text{ cm}^3 \cdot \text{kg}^{1/2} \cdot \text{mol}^{-3/2}$							
300.13	15.07	0.8300	0.1332	-4.1830	69.61	-10.71	93.20 ± 0.10
300.13	15.07	0.5991	0.0986	-3.2196	65.20	-10.94	88.67 ± 0.09
300.23	15.14	0.4973	0.0670	-2.7374	63.96	-9.19	83.01 ± 0.11
300.32	15.15	0.5028	0.0677	-2.7689	63.88	-9.20	82.92 ± 0.08
300.11	15.07	0.2968	0.0506	-1.7924	55.82	-11.26	78.51 ± 0.07
300.09	15.07	0.1954	0.0337	-1.2417	51.19	-11.37	73.34 ± 0.07
$t = (325.11 \pm 0.08)^\circ\text{C}; p = (15.10 \pm 0.04) \text{ MPa}; A_V = 198.00 \text{ cm}^3 \cdot \text{kg}^{1/2} \cdot \text{mol}^{-3/2}$							
325.10	15.07	0.8300	0.1332	-5.5030	37.98	-21.42	68.94 ± 0.10
325.09	15.08	0.5991	0.0986	-4.2978	28.78	-21.88	59.00 ± 0.09
325.20	15.14	0.4973	0.0670	-3.7009	23.33	-18.38	47.33 ± 0.07
325.22	15.16	0.5028	0.0677	-3.7535	22.86	-18.36	46.77 ± 0.10
325.04	15.07	0.2968	0.0506	-2.4526	9.36	-22.50	37.29 ± 0.09
325.04	15.07	0.1954	0.0337	-1.7322	-1.80	-22.72	24.53 ± 0.09

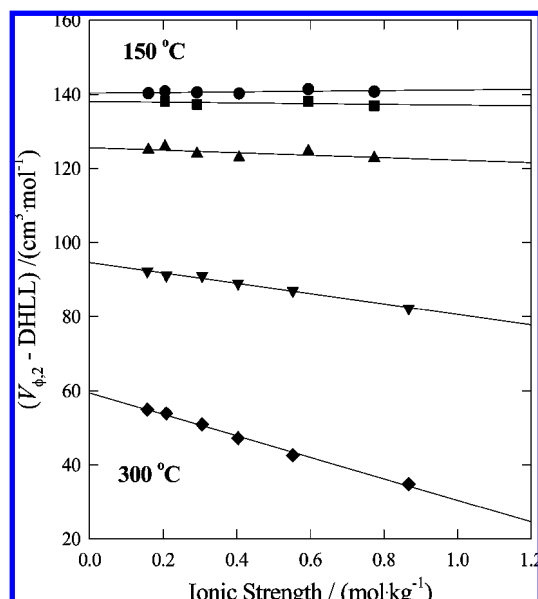


Figure 4. Apparent molar volumes, $V_{\phi,2}$, of aqueous 2-diethylethanolammonium chloride (2-DEEAH⁺Cl⁻) from 150 to 300 °C plotted as a function of ionic strength after subtracting the Debye-Hückel limiting law term (DHLL). Symbols are experimental results, and lines represent the isothermal least-squares fits of eq 7. ● at 150 °C, ■ at 200 °C, ▲ at 250 °C, ▼ at 275 °C and ◆ at 300 °C.

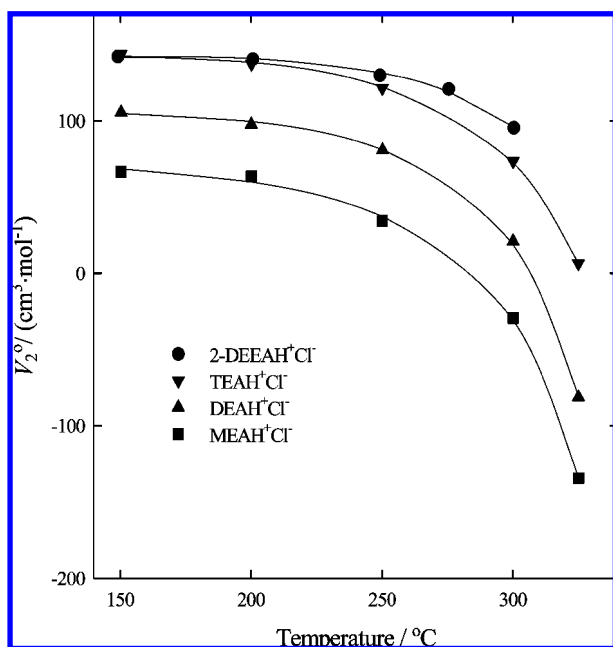


Figure 5. Standard partial molar volumes, V_2^o , of monoethanolammonium chloride (MEA H⁺Cl⁻), diethanolammonium chloride (DEAH⁺Cl⁻), triethanolammonium chloride (TEAH⁺Cl⁻), and 2-diethylethanolammonium chloride (2-DEEAH⁺Cl⁻) plotted as a function of temperature. The lines represent global fit of eq 15 and, symbols are experimental results.

et al.⁴⁶ at temperatures up to 30 °C. Maham et al.⁴⁷ have measured the molar heat capacities of liquid MEA, DEA, TEA, EAE, 2-DEEA, and DMEA at temperatures between 25 and 125 °C.

4. Functional Group Additivity

4.1. Selection of Models for Hydrothermal Conditions. The underlying principle of most functional group additivity models,^{8–10} is that the standard partial molar volume of any

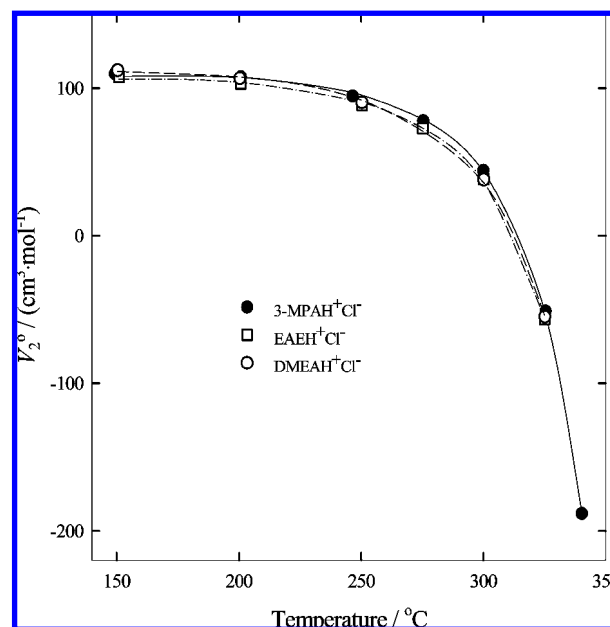


Figure 6. Standard partial molar volumes, V_2^o , of 3-methoxypropylammonium chloride (3-MPAH⁺Cl⁻), ethylethanolammonium chloride (EAEH⁺Cl⁻), and *N,N*-dimethylethanolammonium chloride (DMEA H⁺Cl⁻) plotted as a function of temperature. The lines represent global fits of eq 15, and symbols are experimental results.

solute may be represented by the general equation

$$V_2^o = V_{ss}^o + \sum n_i V_{2,i}^o + \Delta V_{pol}^o \quad (8)$$

where $V_{2,i}^o$ is the contribution of functional group “*i*”; n_i is the number of occurrences of each specific functional group in a given compound; and $V_{ss}^o = \kappa_1^* RT$ is the standard state term, which is the property associated with the transfer of a point mass from the gas phase to the solute standard state.^{32,48} The term ΔV_{pol}^o , which accounts for long-range solvent polarization effects due to ionic charge and dipole moment of the entire solute molecule,⁴⁹ is increasingly important at temperatures above 250 °C. It is omitted in most functional group additivity treatments of neutral species, so that the standard partial molar volume may therefore be represented by the equation

$$V_2^o = V_{ss}^o + \sum n_i V_{2,i}^o \quad (9)$$

Clearly, such models include the assumptions that the contribution of each functional group, $V_{2,i}^o$, does not depend on where it is located on the molecule, and that differences in the long-range solvent polarization are negligible.

Several equations of state for standard partial molar properties have been used as the basis of functional group additivity models for standard partial molar volumes.^{1–7,29} The model used in this work is based on the work of O’Connell,⁵⁰ which is derived from fluctuation solution theory (FST). The O’Connell equation incorporates two aspects of the limiting behavior of solute–solvent interactions in the supercritical region. At the critical point itself, the limiting partial molar properties are described by the generalized Krichevskii equation^{14,15,32}

$$V_2^o = A_{12} \rho_1^* \kappa_1^* RT \quad (10)$$

where A_{12} , the dimensionless Krichevskii parameter, is a well-behaved function, ρ_1^* is the density of water, and κ_1^* is the isothermal compressibility of water, which is discontinuous at the critical point. In the dilute gas limit, the nonideality of a

TABLE 11: Standard Partial Molar Volumes, V_2° , for Aqueous Alkanolammonium and Alkoxyammonium Chlorides Obtained Using Equation 7

t °C	V_2° (cm ³ ·mol ⁻¹) ^a	B_V (cm ³ ·kg·mol ⁻²) ^a	t °C	V_2° (cm ³ ·mol ⁻¹) ^a	B_V (cm ³ ·kg·mol ⁻²) ^a
ethylethanolammonium chloride (EAEH ⁺ Cl ⁻)			2-diethylethanolammonium chloride (2-DEEAH ⁺ Cl ⁻)		
150.91	107.59 ± 0.19	-2.67 ± 0.27	149.16	142.26 ± 0.55	-1.75 ± 1.17
200.77	102.97 ± 0.31	-4.88 ± 0.44	200.74	140.57 ± 1.69	-4.74 ± 3.34
250.36	88.42 ± 0.92	-9.96 ± 1.31	249.21	129.92 ± 1.21	-9.24 ± 2.61
275.25	72.76 ± 1.01	-17.29 ± 1.44	275.50	120.88 ± 0.80	-17.64 ± 1.29
300.16	38.38 ± 0.99	-30.52 ± 1.41	300.40	95.55 ± 1.88	-33.44 ± 3.03
325.10	-56.53 ± 4.05	-71.80 ± 5.79			
3-methoxypropylammonium chloride (3-MPAH ⁺ Cl ⁻)			dimethylethanolammonium chloride (DMEA ⁺ Cl ⁻)		
149.30	109.74 ± 1.40	-1.52 ± 2.09	150.43	112.13 ± 1.94	-8.49 ± 3.79
200.75	107.72 ± 0.81	-5.09 ± 1.19	200.35	106.73 ± 1.78	-10.57 ± 3.49
246.47	94.64 ± 0.72	-9.73 ± 1.07	250.29	90.31 ± 1.95	-13.23 ± 3.82
275.36	77.76 ± 0.87	-17.63 ± 1.30	300.17	38.13 ± 4.67	-31.93 ± 7.66
299.98	44.25 ± 0.71	-31.87 ± 1.07	325.11	-54.88 ± 9.44	-76.05 ± 6.32
325.43	-51.11 ± 5.72	-76.86 ± 8.55			
340.25	-188.18 ± 20.87	-126.50 ± 31.19			
monoethanolammonium chloride (MEA ⁺ Cl ⁻)			diethanolammonium chloride (DEAH ⁺ Cl ⁻)		
150.35	66.74 ± 0.30	-1.19 ± 0.52	150.36	105.65 ± 0.85	-2.43 ± 1.61
200.17	63.79 ± 1.04	-13.50 ± 1.86	200.17	97.77 ± 1.09	-2.28 ± 2.07
250.14	34.27 ± 1.56	-2.61 ± 1.54	250.18	80.83 ± 1.94	-9.15 ± 4.03
300.14	-29.16 ± 5.23	-24.26 ± 9.13	300.12	21.07 ± 0.58	-26.50 ± 0.91
325.14	-134.43 ± 6.56	-73.25 ± 11.45	325.09	-81.22 ± 3.66	-65.80 ± 6.18
triethanolammonium chloride (TEAH ⁺ Cl ⁻)					
150.34	143.80 ± 1.13	-2.82 ± 0.91			
200.22	137.44 ± 0.54	-2.88 ± 0.98			
250.11	121.45 ± 4.05	-5.47 ± 3.27			
300.11	73.51 ± 2.43	-13.71 ± 3.87			
325.06	6.49 ± 5.40	-61.00 ± 18.89			

^a Error limits correspond to standard deviations.

two-component supercritical fluid is described by the virial expansion

$$V_2^\circ = a\rho_1^* + b\rho_1^{*2} + c\rho_1^{*3} + \dots \quad (11)$$

Here, the adjustable parameters a , b , and c are related to the second virial coefficient, and the second and third cross-virial coefficients, respectively. O'Connell⁵⁰ combined eq 10 with the second cross virial coefficient term from eq 11 to obtain the relationship

$$V_2^\circ = V_{ss}^\circ + \{a\rho_1^* + b[\exp(\nu\rho_1^*) - 1]\}\kappa_1^*RT \quad (12)$$

The pressure dependence of V_2° is described implicitly through the density and isothermal compressibility of the solvent. Although it is based on a model for near-critical behavior with parameters derived from a limited data set of low-molecular weight solutes, the O'Connell model has proved to be quite successful over a wide range of temperatures. Its limitations become apparent at temperatures below 150 °C where short-range hydration is important and when applied to large molecules. The O'Connell model served as the basis for a more complex expression derived by Sedlbauer et al.⁴

$$V_2^\circ = V_{ss}^\circ + d(V_1^\circ - \kappa_1^*RT) + \rho_1^*\kappa_1^*RT[a + b\{\exp(\nu\rho_1^*) - 1\} + c \exp(\theta/T) + \delta\{\exp(\lambda\rho_1^*) - 1\}] \quad (13)$$

where ρ_1^* and κ_1^* are the density and isothermal compressibility of water, V_1° is the molar volume of water, V_{ss}° is the standard partial molar volume arising from difference in standard states between the gas phase and solution. The terms $\theta = 1500$ K, $\lambda = -10$ cm³·g⁻¹, and $\nu = 5$ cm³·g⁻¹ are coefficients that do not depend on the solute, while the coefficient δ has the values $\delta = 0.35a$ for nonelectrolytes, $\delta = 0$ for cations and $\delta = -645$ cm³·g⁻¹ for anions. Equation 12 was developed by O'Connell

to describe the classical near-critical behavior of a small collection of inorganic and organic solutes for which data were known in the mid 1990s. The additional exponential parameters δ and λ were added to improve the fit to low-density, high-temperature data for a much larger number of organic solutes. The d term was added to provide a better fit to large solutes in the low temperature, high-density region.

The Yezdimer–Sedlbauer–Wood (YSW) functional group additivity model¹⁰ is based on eq 13 with additional terms for the single-ion charge convention. The standard partial molar volume of each group “ i ” is given by

$$V_{2,i}^\circ = d_i(V_1^\circ - \kappa_1^*RT) + \rho_1^*\kappa_1^*RT[a_i + b_i\{\exp(\nu\rho_1^*) - 1\} + c_i \exp(\theta/T) + \delta_i\{\exp(\lambda\rho_1^*) - 1\}] \quad (14)$$

where a_i , b_i , c_i , and d_i are functional group-specific adjustable parameters. Equation 14 has proved to be well suited to correlate V_2° for a large number of neutral solutes at temperatures up to 250 °C and has been extended to treat electrolytes. Our experimental results for 2- and 3-hydroxypropionic acid²⁷ and MEA (Tables 6 and 11) at $t \leq 250$ °C agree with the YSW predictions to within 3 cm³·mol⁻¹. The model's predictions for these solutes at higher temperatures become increasingly too negative, yielding the wrong sign for the critical-point divergence. Not surprisingly, it does not work well for glycolic acid and tartaric acid, which contain closely packed polar groups.²⁶ Also, the model does not include the ≥N and >NH functional groups.

We note that Criss and Wood⁸ and Inglese et al.⁵¹ have reported equations for functional group contributions to V_2° and $C_{p,2}^\circ$ at temperatures up to 250 °C, but their equations cannot be extrapolated to higher temperatures and are limited to the 28 MPa isobar. The existing high-temperature group additivity models for V_2° were less accurate above 250 °C because they

TABLE 12: Parameters Obtained from Equation 15 for the Organic Solutes^a

	$a/(\text{cm}^3\cdot\text{g}^{-1})$	$b/(\text{cm}^6\cdot\text{g}^{-2})$	c
acetic acid ^b	-11.90 ± 0.35	0	0.39 ± 0.01
methanol ^c	5.23 ± 1.32	-23.59 ± 2.31	0.35 ± 0.01
ethanol ^c	7.06 ± 1.72	-31.79 ± 3.00	0.50 ± 0.01
1-propanol ^c	6.29 ± 2.01	-35.48 ± 3.51	0.63 ± 0.01
2-propanol ^c	8.89 ± 2.17	-39.90 ± 3.78	0.65 ± 0.01
hydracrylic acid (3-hydroxypropionic acid)	22.46 ± 1.85	-73.37 ± 3.72	0.78 ± 0.02
monoethanolamine (MEA)	23.75 ± 1.35	-68.78 ± 2.74	0.67 ± 0.01
diethanolamine (DEA)	21.53 ± 1.70	-79.32 ± 3.46	0.96 ± 0.02
triethanolamine (TEA)	26.46 ± 2.82	-103.91 ± 5.75	1.30 ± 0.03
ethylethanolamine (EAE)	11.50 ± 7.41	-50.59 ± 15.24	0.81 ± 0.07
2-diethylethanolamine (2-DEEA)	68.33 ± 1.29	-153.70 ± 2.39	1.35 ± 0.01
<i>N,N</i> -dimethylethanolamine (DMEA)	17.31 ± 1.94	-64.14 ± 3.99	0.88 ± 0.02
3-methoxypropylamine (3-MPA)	46.13 ± 3.03	-118.75 ± 6.75	1.11 ± 0.04
ethylethanolammonium chloride (EAEH ⁺ Cl ⁻)	-13.16 ± 4.79	-55.89 ± 9.84	1.09 ± 0.05
2-diethylethanolammonium chloride (DEEAH ⁺ Cl ⁻)	25.92 ± 13.22	-133.88 ± 24.48	1.56 ± 0.09
3-methoxypropylammonium chloride (3-MPAH ⁺ Cl ⁻)	-21.56 ± 2.99	-39.85 ± 6.65	1.04 ± 0.04
sodium hydracrylate (sodium 3-hydroxypropionate)	44.25 ± 8.96	-138.00 ± 18.45	1.00 ± 0.08
monoethanolammonium chloride (MEA ⁺ Cl ⁻)	0	-73.32 ± 1.31	0.93 ± 0.02
diethanolammonium chloride (DEA ⁺ Cl ⁻)	0	-85.20 ± 0.81	1.21 ± 0.01
triethanolammonium chloride (TEA ⁺ Cl ⁻)	33.70 ± 4.22	-157.36 ± 8.59	1.70 ± 0.04
<i>N,N</i> -dimethylethanolammonium chloride (DMEA ⁺ Cl ⁻)	0	-84.05 ± 0.74	1.23 ± 0.01

^a Error limits correspond to standard errors. ^bMajer et al.¹⁹ ^cHynčica et al.²⁰

were developed using only literature data up to 250 °C. Another group additivity model for neutral organic solutes, reported by Amend and Helgeson,⁹ is based on the HKF equation of state, which was developed from a theoretical framework for ionic solvation.^{32,35} As such, the Criss–Wood and Amend–Helgeson group additivity models are purely empirical fits to experimental data.

4.2. Correlation of Standard Partial Molar Volume Data.

The objective of this work was to explore the validity of the functional group additivity approach to temperatures well above the current limit of 250 °C, into the region where models based on the limiting near-critical Krichevskii behavior should apply. Our approach was to combine the new experimental values of V_2^0 in Tables 6 and 11 with recently published data for carboxylic acids and alcohols^{19,20} to derive the contributions of structural groups found in oxygen- and nitrogen-containing organic compounds: $-\text{CH}_3$, $-\text{CH}_2$, $-\text{CH}$, $-\text{OH}$, $-\text{COOH}$, $-\text{O}-$, $>\text{N}$, $>\text{NH}$, $-\text{NH}_2$, $-\text{COO}^-\text{Na}^+$, $-\text{NH}_3^+\text{Cl}^-$, $>\text{NH}_2^+\text{Cl}^-$, and $>\text{NH}^+\text{Cl}^-$. Because the focus of this work is on the high-temperature limiting behavior of V_2^0 , our database and modeling efforts were restricted to temperatures above 150 °C, so that complications associated with low-temperature “structural” hydration effects could be avoided.

At the onset of this study, we had expected that the simple 2-parameter O’Connell expression, eq 12, would have represented the high-temperature data adequately at least at temperatures above 250 °C. This was not found to be the case and several alternative expressions were tried, including the alternative form of the O’Connell expression,⁵² the various “density” models used by Criss and Wood,⁸ and the YSW model,¹⁰ eq 13, without the low-temperature d term and using the exponential terms as adjustable parameters. The most successful simple model was found to be a modified form of O’Connell’s 1995 equation,⁵⁰ in which a term similar in form to the third cross-virial coefficient from eq 11 is included

$$V_2^0 = V_{ss}^0 + \{a\rho_1^* + b\rho_1^{*2} + c[\exp(v\rho_1^*) - 1]\}\kappa_1^*\cdot R\cdot T \quad (15)$$

Here, ρ_1^* is the density of water; κ_1^* is the isothermal compressibility of water, $v = 0.005 \text{ m}^3\cdot\text{kg}^{-1} = 5 \text{ cm}^3\cdot\text{g}^{-1}$ is a constant, which replaces the value $v = 0.0055 \text{ m}^3\cdot\text{kg}^{-1}$ derived

by O’Connell⁵⁰ from fitting eq 12 to data for a number of simple solutes. The constants a , b , and c are solute-specific adjustable parameters. The standard state term for neutral species, $V_{ss}^0 = \kappa_1^*RT$, must be doubled for the chloride and sodium salts, so that $V_{ss}^0 = 2\kappa_1^*RT$ for the functional groups $-\text{COO}^-\text{Na}^+$, $-\text{NH}_3^+\text{Cl}^-$, $>\text{NH}_2^+\text{Cl}^-$, and $>\text{NH}^+\text{Cl}^-$. The advantage of eq 15 is that it is simple and requires fewer parameters than the YSW model. The added density term, $b\rho_1^{*2}$, significantly improved the description of the standard partial molar volumes of our compounds. Although it is consistent with the third cross-virial coefficient of the solute and steam at low-pressure supercritical limit, the magnitude of the b parameter from least-squares fits leads us to believe it serves purely as a fitting parameter. Equation 15 was fitted by a nonlinear least-squares method to values of V_2^0 for the alkanolamines and the alkoxyamine and their salts listed in Tables 6 and 11. The equation of state parameters for each individual solute were determined empirically by using a least-square procedure to fit eq 15 to the experimental values of V_2^0 . In addition to fitting our own measurements, parameters were also determined from V_2^0 data for acetic acid ($150 \text{ °C} \leq t \leq 300 \text{ °C}$; $10 \text{ MPa} \leq p \leq 37 \text{ MPa}$) reported by Majer et al.,¹⁹ methanol, ethanol, 1-propanol, and 2-propanol ($150 \text{ °C} \leq t \leq 300 \text{ °C}$; $p \leq 30 \text{ MPa}$) from recent measurements by Hynčica et al.,²⁰ and our own results for 3-hydroxypropanoic acid.²⁷ In most cases, the fits agreed with experiment to within $\pm 2 \text{ cm}^3\cdot\text{mol}^{-1}$. This compares with the original 2-parameter O’Connell model, eq 12 and its variations, for which standard errors of up to $\pm 6 \text{ cm}^3\cdot\text{mol}^{-1}$ were observed with maximum deviations as high as $\pm 10 \text{ cm}^3\cdot\text{mol}^{-1}$ at the highest temperature. The fits to data for the alcohols and acetic acid for which pressure-dependent data are available showed much larger deviations for the high-pressure data points, typically $+3 \text{ cm}^3\cdot\text{mol}^{-1}$ at 30 MPa. The largest discrepancies observed for our own data were for ethylethanolamine (EAE), which had a maximum deviation of $+4 \text{ cm}^3\cdot\text{mol}^{-1}$ at 300 °C if the data point at 325 °C was included in the fit. The maximum deviation observed for other solutes was less than $\pm 2 \text{ cm}^3\cdot\text{mol}^{-1}$. The fitted parameters are tabulated in Table 12, along with their standard errors and the source of data. Deviations between the fitted and experimental values are listed in Table 13. These equation of state parameters were then used

TABLE 13: Difference of the Experimental Values of the Partial Molar Volumes from Calculations by Equation 15 and the Group Additivity Model from This Work

<i>t</i> °C	δV_2^o (fit) ^a (cm ³ ·mol ⁻¹)	δV_2^o (model) ^b (cm ³ ·mol ⁻¹)	δV_2^o (fit) (cm ³ ·mol ⁻¹)	δV_2^o (model) (cm ³ ·mol ⁻¹)	δV_2^o (fit) (cm ³ ·mol ⁻¹)	δV_2^o (model) (cm ³ ·mol ⁻¹)
monoethanolamine (MEA)			diethanolamine (DEA)		triethanolamine (TEA) ^c	
150	-0.14	-0.14	0.48	2.25	0.78	3.02
200	-0.13	-0.13	-0.38	1.86	-0.59	6.12
250	0.50	0.50	-0.34	1.84	-0.62	10.46
300	-0.34	-0.35	0.39	-1.28	0.67	4.98
325	0.09	0.08	-0.11	-12.62	-0.19	-32.90
ethylethanolamine (EAE)			2-diethylethanolamine (2-DEEA) ^c		dimethylethanolamine (DMEA)	
150	1.68	0.49	-0.13	-3.20	0.41	0.42
200	-0.18	-1.72	0.22	-3.59	-0.15	-0.13
250	-2.39	-3.66	-0.10	-0.61	-0.97	-0.95
275	-1.61	-1.84	-0.01	7.18	0.71	0.73
300	3.44	6.41	0.02	27.35	0.10	0.13
325	-0.83	13.50			-0.08	-0.03
3-hydroxypropionic acid			3-methoxypropylamine			
100	0.40	1.06				
150	-0.40	-0.40	-1.63	-0.95		
200	-0.17	-1.04	-0.14	-0.67		
250	0.18	0.28	1.65	1.16		
275	0.25	0.06	2.41	2.59		
300	-0.82	-0.33	-2.38	-1.66		
315	0.84	0.95				
325	-0.24	-0.49	-0.48	-0.75		
340			0.43	0.64		

^a δV_2^o (model) = V_2^o (exp) - V_2^o (calc), group additivity model, eq 9. ^b δV_2^o (fit) = V_2^o (exp) - V_2^o (calc), fitting, (eq 15). ^c TEA and 2-DEEA data were not used to fit group additivity parameter in the model.

as the basis for the development of our group additivity model. The expression corresponding to eq 15 for $V_{2,i}^o$, the standard partial molar volume of each functional group i , is

$$V_{2,i}^o = \{a_i \rho_1^* + b_i \rho_1^{*2} + c_i [\exp(v \rho_1^*) - 1]\} \kappa_1^* RT \quad (16)$$

The parameters a , b , and c from Table 12 were decomposed to obtain the group contributions a_i , b_i , and c_i . The effect of pressure is determined through the density and compressibility of water, ρ_1^* and κ_1^* , respectively. Because the number of neutral solutes (13) is only marginally larger than the number of functional groups (9), almost all of the experimental parameters are required to determine the functional group contributions.

The first phase of this procedure used values of V_2^o for acetic acid, methanol, ethanol, 1-propanol, 2-propanol, and 3-hydroxypropanoic acid to determine additivity parameters for the functional groups -CH₃, >CH₂, >CH-, -OH, and -COOH. The fit was restricted to temperatures in the range 150 °C ≤ t ≤ 300 °C and pressures, p ≤ 30 MPa. The second phase of the procedure then used the fitted values for a_i , b_i , and c_i of these functional groups to determine additivity parameters for the functional groups -O-, -NH₂, >NH, and >N- based on the values of a , b , and c for MEA, EAE, DEA, DMEA, and 3-MPA from Table 12. The temperature range used in the fit was 150 °C ≤ t ≤ 325 °C, except for 3-MPA (150 °C ≤ t ≤ 340 °C). The consequence of these upper temperature limits is that with the exception of >NH the values for all these groups above 300 °C are based on data for only one solute molecule and on extrapolated values for the alkyl groups. Values of the fitted functional group parameters are tabulated in Table 14. The corresponding values of $V_{2,i}^o$, calculated from them, are plotted in Figures 7 and 8.

There are a limited number of experimental values for V_2^o of other species with which to test this model. The results for glycolic acid,²⁶ 2-hydroxypropionic acid (lactic acid),²⁷ and TEA were not used to derive the functional-group additivity param-

TABLE 14: Functional Group Parameters for Aqueous Organic Solutes According to Equation 16^a

	a_i /(cm ³ ·g ⁻¹)	b_i /(cm ⁶ ·g ⁻²)	c_i
-CH ₃	-11.40 ± 0.89	14.28 ± 1.55	0.14 ± 0.01
-CH ₂	0.53 ± 0.38	-5.95 ± 1.30	0.14 ± 0.01
-CH	14.63 ± 1.63	-29.84 ± 2.83	0.15 ± 0.01
-OH	17.06 ± 1.39	-38.62 ± 2.40	0.22 ± 0.01
-COOH	4.34 ± 0.89	-22.86 ± 1.55	0.28 ± 0.01
-NH ₂	5.62 ± 1.39	-18.27 ± 2.40	0.18 ± 0.01
>NH	-5.23 ± 3.36	6.65 ± 5.34	0
>N-	21.99 ± 4.76	-42.18 ± 7.56	0.11 ± 0.02
-O-	49.29 ± 20.75	-94.55 ± 34.77	0.36 ± 0.10
-COO ⁻ Na ⁺	26.13 ± 9.72	-87.49 ± 17.94	0.51 ± 0.07
-NH ₃ ⁺ Cl ⁻	-39.58 ± 6.87	17.73 ± 12.69	0.28 ± 0.05
>NH ₂ ⁺ Cl ⁻	-28.33 ± 6.87	0	0.27 ± 0.05
>NH ⁺ Cl ⁻	0	-62.10 ± 17.94	0.46 ± 0.07

^a Error limits correspond to standard errors.

eters because they contain closely spaced polar groups. The V_2^o results for 2-DEEA were not used because of the possibility of decomposition at 300 °C. In addition, values for several alcohols⁵³⁻⁵⁶ have been published since this work was done. The deviations of the group additivity model predictions from the experimental data used in the fit and these independent results are plotted in Figures 9 and 10.

Values of the group additivity parameters for the ionic groups, -COO⁻Na⁺, -NH₃⁺Cl⁻, >NH₂⁺Cl⁻, and >NH⁺Cl⁻, were determined from the a , b , and c parameters for the corresponding salts in Table 12 and the fitted parameters for the neutral functional groups. They are tabulated in Table 14. We know of no other experimental values of V_2^o for alkanolamines at temperatures above 250 °C with which to test the model.

5. Discussion

5.1 Functional Group Additivity at Elevated Temperatures. The functional group contributions to V_2^o , which are shown in Figures 7 and 8, undergo marked changes in their temperature dependence above 250 °C. At lower temperatures,

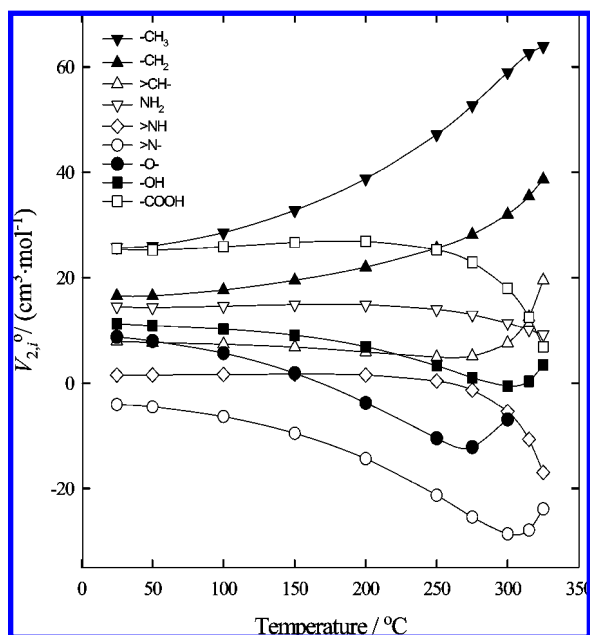


Figure 7. Functional group contributions for neutral species plotted as a function of temperature at saturation pressures, p_{sat} .

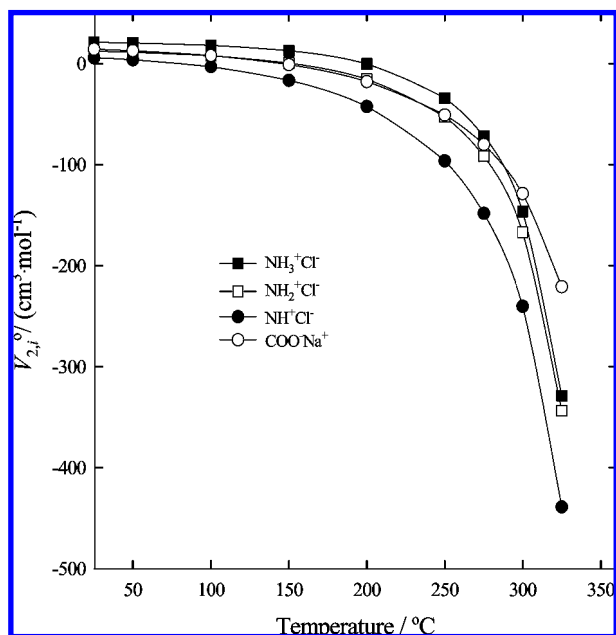


Figure 8. Functional group contributions for salts plotted as a function of temperature at saturation pressures, p_{sat} .

the relative magnitude of $V_{2,i}^0$ for each group is identical to that observed in similar models at room temperature⁵⁷

$$(-\text{CH}_3) \approx (-\text{COOH}) > (>\text{CH}_2) > (-\text{NH}_2) > (-\text{OH}) > (-\text{O}-) > (>\text{CH}-) > (>\text{NH}) > (>\text{N}-)$$

At higher temperatures, the magnitude of $V_{2,i}^0$ for polar groups begins to decrease sharply with increasing temperature while those for nonpolar groups show a corresponding increase. At temperatures above 300 °C, the relative magnitude of the extrapolated values is as follows:

$$(-\text{CH}_3) > (>\text{CH}_2) > (>\text{CH}-) > (-\text{NH}_2) > (-\text{COOH}) > (-\text{OH}) > (>\text{NH}) > (>\text{N}-)$$

The ether group ($-\text{O}-$) is excluded from this list for reasons discussed below. These group additivity contributions include

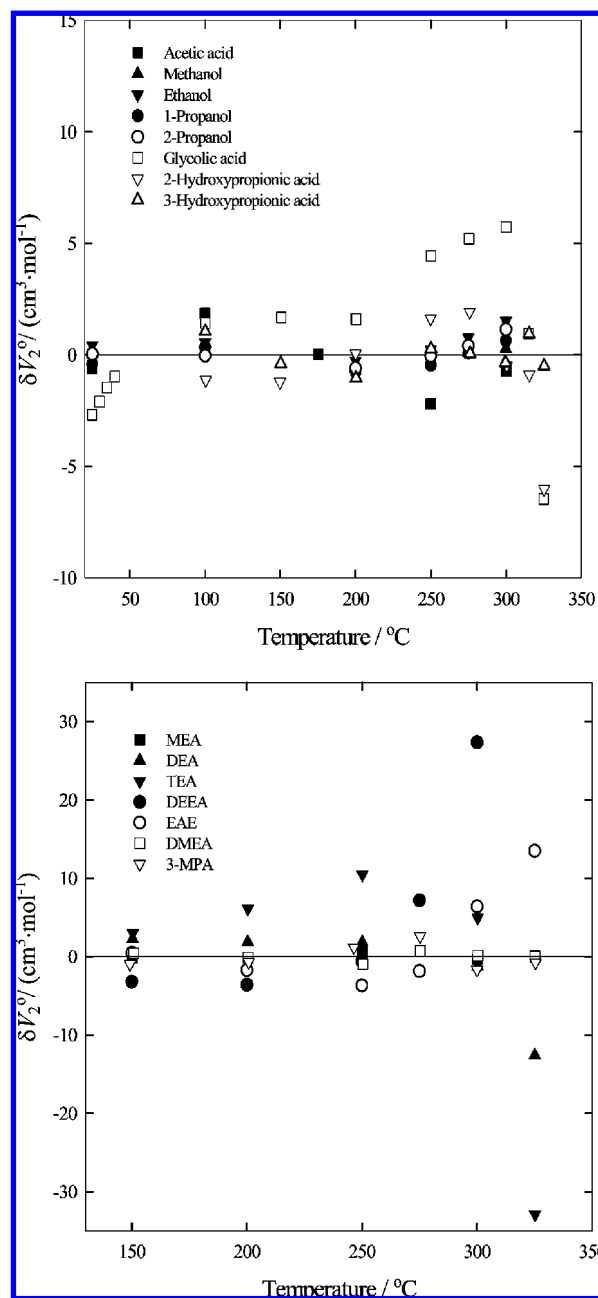


Figure 9. Difference plots showing $\delta V_{2,i}^0 = V_{2,i}^0(\text{exp}) - V_{2,i}^0(\text{model})$, the experimental standard partial molar volume of (a) carboxylic acids and alcohols (b) alkoxy- and alkanolamines, relative to the values calculated using functional group additivity model from this work at pressures near 15 MPa. The values for glycolic acid, 2-DEEA, and TEA were not used to derive the functional group parameters.

both the intrinsic volume of the functional group and short-range localized hydration effects. The contribution for the nonpolar groups $-\text{CH}$, $-\text{CH}_2$, and $-\text{CH}_3$ become increasingly positive with temperature as one might expect for nonpolar species in which hydrophobic hydration effects dominate. The $-\text{O}-$ and $>\text{N}-$ groups show a decrease in $V_{2,i}^0$ with increasing temperature then behave in similar fashion by swinging sharply to increasingly positive values above 250 °C. If true, this behavior is particularly interesting because these groups are shielded from hydration effects by their substituent functional groups. It is also possible that their change in behavior above 300 °C is the result of undetected thermal decomposition in 3-MPA and DMEA. The behavior of the ether group ($-\text{O}-$) is so extreme that we believe decomposition of 3-MPA must have

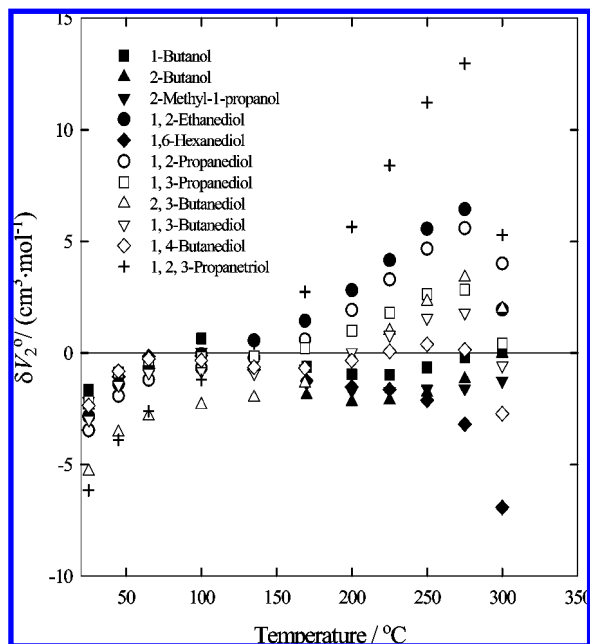
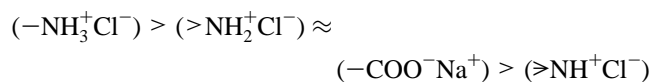


Figure 10. Difference plots showing $\delta V_2^0 = V_2^0(\text{exp}) - V_2^0(\text{model})$, the experimental standard partial molar volume of butanols and polyhydric alcohols from Hycicia et al.^{53–55} and Cibulka et al.⁵⁶ relative to the values calculated using functional group additivity model from this work at 15 MPa. None of these data were used to derive the functional group parameters.

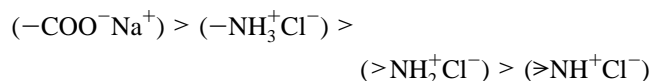
taken place. At temperatures above 250 $^\circ\text{C}$, the standard partial molar volumes of the polar groups $-\text{COOH}$, $-\text{OH}$, $-\text{NH}_2$, and $>\text{NH}$ decrease toward negative values, as might be expected if short-range solvent hydrophilic effects become more important due to the increasing compressibility of liquid water. The modest upswing in $V_{2,i}^0$ for the $(-\text{OH})$ group above 300 $^\circ\text{C}$ may be an artifact.

We note Yezdimer et al.¹⁰ reported values of $V_{2,i}^0$ for the $(-\text{CH})$ group that swing toward negative values above 250 $^\circ\text{C}$, and that Criss and Wood⁸ reported values of $V_{2,i}^0$ for the $-\text{OH}$ and $-\text{NH}_2$ group whose temperature dependence also shifts from negative to positive at $t \geq 200$ $^\circ\text{C}$. Both models are heavily based on the experimental measurements of Criss and Wood,⁸ which extend only to 250 $^\circ\text{C}$. Our measurements at higher temperatures do not support these conclusions.

All electrolytes studied to date exhibit negative Krichvskii parameters,³² and this behavior is illustrated by the group additivity parameters for the salts, shown in Figure 8. At 150 $^\circ\text{C}$, the functional group contributions for the salts follow the order



consistent with room temperature behavior.^{8–10,57} At 300 $^\circ\text{C}$, the $V_{2,i}^0$ terms plunge toward much more negative values and follow the order



The more positive value for the $(-\text{COO}^-\text{Na}^+)$ group at the highest temperatures is consistent with long-range polarization effects, which dominate at these temperatures. These can be approximated by the Born equation^{2,32,58} and are strongest for

ions with the smallest effective radii. The effective radius of the hydrated Na^+ cation is similar to that of the weakly hydrated Cl^- anion,² so that the group contributions appear to follow the order of their intrinsic volumes with the larger carboxylate group followed by the contributions of the amine groups according to the order of their van der Waals radii.

5.2. Predicted Standard Partial Molar Volumes. The results in Table 13 show that the proposed functional group additivity model yields reasonable agreement with experimental values over a wide range of temperatures from 150 up to 300 $^\circ\text{C}$ for organic solutes from which the contributions $V_{2,i}^0$ were derived. The model deviates from literature values for the alkanols and carboxylic acids by less than 3 $\text{cm}^3 \cdot \text{mol}^{-1}$ at temperatures below 300 $^\circ\text{C}$, which is the highest temperature reported. A plot of the differences is presented in Figure 9a. The deviations between the model and experimental values for the alkanolamines are plotted in Figure 9b. With the exception of 2-DEEA and TEA, which were not used in the fit, the predicted and measured values of V_2^0 for the alkanolamines agree to within ± 5 $\text{cm}^3 \cdot \text{mol}^{-1}$.

A rigorous test of the model's success is to compare those results with V_2^0 for solutes that were not used in the derivation of the group additivity model. These include 2-DEEA and TEA plotted in Figure 9b, 2-hydroxypropionic acid, glycolic acid, and tartaric acid in Figure 9a, and the newly reported alkanols, alkanediols, and alkanetriols in Figure 10.^{53–56} At 300 $^\circ\text{C}$, 2-DEEA is close to its decomposition temperature, and the experimental results are suspect. The discrepancy in the results for TEA at 325 $^\circ\text{C}$ is anomalous, because decomposition products were only observed at temperatures above 325 $^\circ\text{C}$ and the experimental results should be accurate. Although the group-additivity model does predict V_2^0 for most of the alkanols plotted in Figure 10 to within ± 5 $\text{cm}^3 \cdot \text{mol}^{-1}$, clearly there are systematic differences for 1,2-ethanediol, 1,2-propanediol, and especially 1,2,3-propanetriol. The experimental values for these molecules exceed the model predictions at temperatures up to 250 $^\circ\text{C}$, then plunge sharply at 300 $^\circ\text{C}$ in a manner similar to glycolic acid, as discussed below.

A plot comparing experimental and predicted values V_2^0 for 2- and 3-hydroxypropionic acid is given in Figure 11. With the exception of the data point at 325 $^\circ\text{C}$, the group-additivity values of data for 2-hydroxypropionic acid agree with the measured values of V_2^0 to within 2 $\text{cm}^3 \cdot \text{mol}^{-1}$. The small systematic difference between the two isomers is due to differences in the contribution of two $(>\text{CH}_2)$ groups in 3-hydroxypropionic acid versus one $(-\text{CH}_3)$ + one $(>\text{CH}-)$ group in 2-hydroxypropionic acid. As noted in our earlier paper,²⁷ the predictions of the Yezdimer–Sedlbauer–Wood model are equally good up to 250 $^\circ\text{C}$ but deviate toward much more negative values at higher temperatures. The results for glycolic acid are plotted in Figure 12. The group additivity calculations agree with experiment to within ± 5 $\text{cm}^3 \cdot \text{mol}^{-1}$ up to 300 $^\circ\text{C}$; however, at higher temperatures the model predicts a positive divergence in V_2^0 , and a negative divergence is actually observed. Glycolic acid is a special case, because it is so polar with two polar functional groups on a 1-carbon backbone. The effects of multipole solvent polarization, which can be significant, are discussed below in Section 5.3.

5.3. The Effect of Long-Range Solvent Polarization. One possible cause of the limited success of the group additivity model above 300 $^\circ\text{C}$ is our neglect in eq 8 of the term ΔV_{pol}^0 , which accounts for long-range solvent polarization effects. Lin and Sandler⁵⁹ have attempted to address this problem for the case of Henry's Law constants at room temperature by using

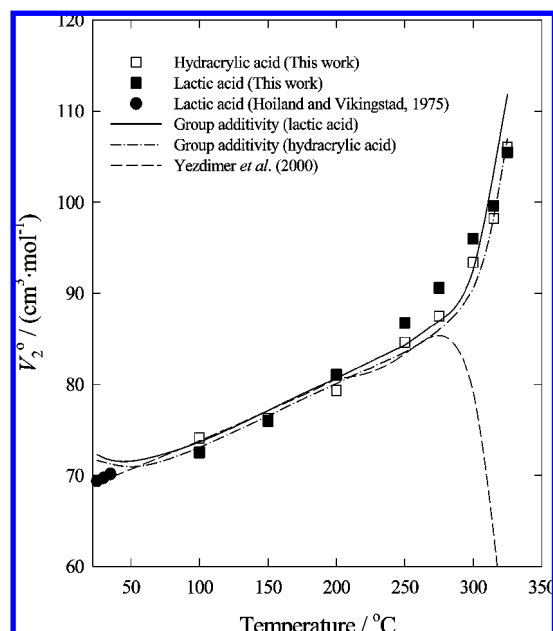


Figure 11. Standard partial molar volumes, V_2^o of lactic and hydracrylic acids plotted as a function of temperature. The lines show the prediction made by extrapolating the functional group additivity model of Yezdimer et al.¹⁰ and our functional group additivity model (eq 16).

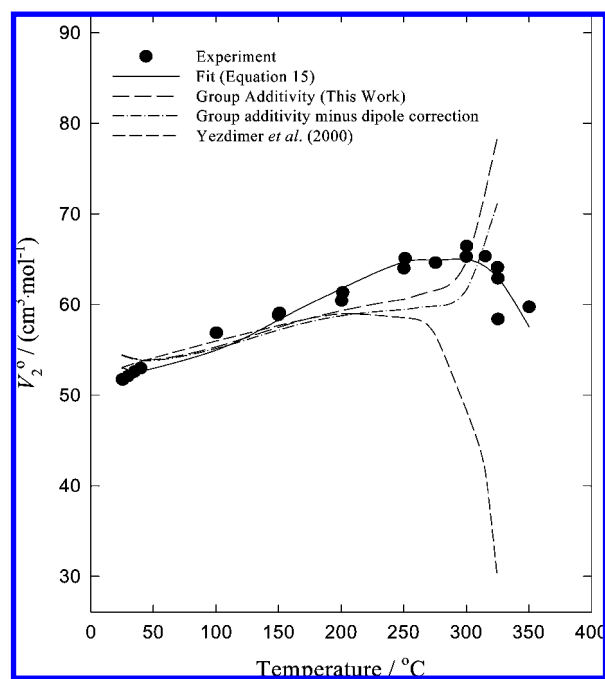


Figure 12. Standard partial molar volumes, V_2^o of glycolic acid plotted as a function of temperature. The lines show the global fit to eq 15 to the experimental data of Bulemela and Tremaine,²⁶ a prediction made by extrapolating the functional group additivity model of Yezdimer et al.,¹⁰ and our functional group additivity model (eq 16) before and after the dipole correction at saturation pressures.

quantum mechanical calculations to determine the charge distribution on each solute molecule for which group additivity calculations are undertaken. The Gibbs energy of polarization was calculated using the charge and dipolar terms in the multipole expansion of the Born equation with a spherical cavity approximation for each functional group. The solvation of organic nonelectrolytes in high-temperature water is expected to be different than that at room temperature, because short-

range hydration effects are less specific and because the high compressibility of liquid water under these conditions causes long-range polarization effects to dominate.⁶⁰ This is particularly important for species that demonstrate hydrophobic behavior consistent with a positive Krichevskii parameter in which water–water interactions cause the solvation sphere to pull away from the solute molecule. In our calculations, we have chosen to use the spherical Onsager approximation to describe the reaction field associated with the net dipole of each solute molecule in calculating ΔV_{pol}^o . The dipole moment and van der Waals radius of the molecule were calculated using the *Gaussian 03* software package (Gaussian Inc., Wallingford, CT) at the restricted Hartree–Fock level of theory, using a full geometry optimization with the 6-31G(d, p) basis set to be consistent with Lin and Sandler.⁵⁹ The Onsager spherical cavity approximation was used in preference to more sophisticated isodensity polarized continuum models because of its simplicity. Moreover, most of these molecules show a net hydrophobic effect which is expected to create an increasingly large cavity volume as the critical point is approached.^{1,14,32} As a result, it is not clear that the isodensity treatments will provide a significant improvement in accuracy for these very approximate calculations under near-critical conditions.

Table 15 lists the dipole moment of each solute molecule, both in the gas phase and in the presence of the Onsager reaction field, the solute radius, r_e , and the standard partial molar volume of polarization, ΔV_{pol}^o , as calculated from the expression⁴⁹

$$\Delta V_{\text{pol}}^o = \{\mu^2 N_A / (4\pi\epsilon_0 r^3)\} [-3/(2\epsilon_r + 1)^2] (\partial\epsilon_r / \partial p)_T \quad (17)$$

Here, μ is the dipole moment of the charge distribution in the spherical cavity, N_A is Avogadro's number, ϵ_r is the static dielectric constant (relative permittivity) of the solvent, ϵ_0 is the permittivity of free space, and r_e is the effective radius of the dissolved species. The calculated dipole moment of the solvated molecule, μ , differs from the gas-phase value, μ_{gas} , and shows a slight temperature dependence because of the role of the dielectric constant in determining the Onsager reaction field. However, the variations in ΔV_{pol}^o primarily reflect the effect of the temperature and pressure dependence of the dielectric constant, ϵ_r , in the dipole term of the Born equation, eq 17. By definition, solvent polarization is always attractive and causes the standard partial molar volume of polarization for the dissolved dipolar species to decrease. As shown in Table 15, the effect increases with temperature, becoming much larger at temperatures and pressures approaching the critical point. Because it ignores the expansion of the cavity for hydrophobic solutes and dielectric saturation effects for hydrophilic solutes, this treatment probably over-predicts the contribution ΔV_{pol}^o . In addition, the calculation does not include the effects of thermal motion, which would also reduce the effective dipole moment. Finally, we note that Wood and his co-workers⁵⁸ have shown that the approximations inherent in the Born equation break down near the critical point due to solvent compressibility effects and that these effects are less serious for dipolar molecules than for ionic species.

The magnitude (absolute values) of ΔV_{pol}^o in Table 15 follows the order

glycolic acid \gg tartaric acid \approx MEA $>$ EAE \approx
2-hydroxypropionic acid

The calculated solvent polarization term for both tartaric acid and MEA is only $-1.5 \text{ cm}^3 \cdot \text{mol}^{-1}$ at 300 °C and $-8 \text{ cm}^3 \cdot \text{mol}^{-1}$ at 350 °C, and it is less for the other alkanolamines. Thus, while

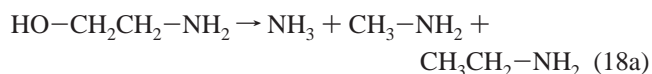
TABLE 15: Dipole Moments, μ , in Solution, Solute Radius, r_e , and the Standard Partial Molar Volume of Polarization, ΔV_{pol}^o

t °C	p MPa	μ (Debye)	ΔV_{pol}^o (cm ³ ·mol ⁻¹)	μ (Debye)	ΔV_{pol}^o (cm ³ ·mol ⁻¹)	μ (Debye)	ΔV_{pol}^o (cm ³ ·mol ⁻¹)
MEA				DEA		TEA	
		$r_e = 3.66 \text{ \AA}, \mu_{\text{gas}} = 2.44$		$r_e = 4.27 \text{ \AA}, \mu_{\text{gas}} = 2.01$		$r_e = 4.48 \text{ \AA}, \mu_{\text{gas}} = 1.16$	
200	15	2.88	-0.24	2.75	-0.14	1.47	-0.03
250	15	2.87	-0.50	2.73	-0.29	1.47	-0.07
300	15	2.86	-1.40	2.72	-0.80	1.46	-0.20
325	15	2.85	-3.13	2.70	-1.77	1.45	-0.44
350	20	2.85	-7.65	2.68	-4.29	1.45	-1.08
EAE				2-DEEA		DMEA	
		$r_e = 4.01 \text{ \AA}, \mu_{\text{gas}} = 2.48$		$r_e = 4.38 \text{ \AA}, \mu_{\text{gas}} = 2.03$		$r_e = 4.14 \text{ \AA}, \mu_{\text{gas}} = 2.21$	
200	15	2.80	-0.18	2.31	-0.09	2.47	-0.12
250	15	2.80	-0.36	2.31	-0.19	2.46	-0.26
300	15	2.79	-1.01	2.30	-0.53	2.46	-0.72
325	15	2.78	-2.26	2.30	-1.18	2.46	-1.61
350	20	2.78	-5.54	2.29	-2.89	2.45	-3.92
2-hydroxypropionic acid				3-hydroxypropionic acid		glycolic acid	
		$r_e = 3.81 \text{ \AA}, \mu_{\text{gas}} = 1.96$		$r_e = 3.72 \text{ \AA}, \mu_{\text{gas}} = 1.39$		$r_e = 3.44 \text{ \AA}, \mu_{\text{gas}} = 3.38$	
200	11	2.36	-0.15	1.92	-0.11	3.86	-0.55
250	11	2.35	-0.32	1.91	-0.22	3.86	-1.16
300	11	2.34	-0.95	1.90	-0.66	3.85	-3.10
325	15	2.34	-1.87	1.89	-1.31	3.84	-7.24
350	20	2.33	-4.54	1.88	-3.17	3.83	-17.90
3-methoxypropylamine				tartaric acid			
		$r_e = 3.94 \text{ \AA}, \mu_{\text{gas}} = 0.61$		$r_e = 4.02 \text{ \AA}, \mu_{\text{gas}} = 2.77$			
200	15	0.74	-0.01	3.44	-0.26		
250	15	0.74	-0.03	3.43	-0.54		
300	15	0.73	-0.07	3.42	-1.51		
325	15	0.73	-0.17	3.42	-3.41		
350	17	0.73	-0.30	3.41	-8.29		

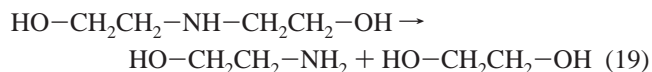
the contribution of ΔV_{pol}^o is significant, it is not enough to account for the variations from group additivity observed above 300 °C. The exception is glycolic acid, which has values of ΔV_{pol}^o ranging from $-3 \text{ cm}^3\cdot\text{mol}^{-1}$ at 300 °C to $-18 \text{ cm}^3\cdot\text{mol}^{-1}$ at 350 °C, because of its small size and large dipole moment. The effect of adding this term to the group additivity prediction from eq 16 is plotted in Figure 12. Although the solvation calculation is very approximate, the results suggest that the negative divergence in the experimental data for glycolic acid is at least partially due to long-range polarization effects. A more sophisticated treatment of hydration effects between glycolic acid and one or two water molecules by Thakkar et al.⁶¹ shows significant hydrogen bonding between the hydroxyl and carboxylic groups in the most stable structures, some of which have a bridging or coordinated water. None of these are represented in our Onsager reaction field treatment.

5.4. Thermal Decomposition Reactions. While the objective of this study was to examine the thermodynamic properties of these systems at temperatures above 250 °C, the decomposition mechanisms of alkanolamines and alkoxyamines under these extreme conditions have not been studied in detail,^{62,63} and the results of our NMR studies on quenched samples merit discussion. In their comprehensive review, Brill and Savage⁶² have noted that alcohols and carboxylic acids undergo acid-catalyzed dehydration and decarboxylation reactions. Amines are less reactive, and less well studied but are known to undergo hydrolysis reactions in parallel with free-radical thermolysis reactions. The thermal degradation of the alkanolamines and alkoxyamine measured in this work is consistent with a mechanism that involves reductive cleavage to form amines and alcohols in a similar manner to the proposed reaction scheme for the decomposition of morpholine by Gilbert and Lamarre.⁶⁴ According to this mechanism, decomposition takes place initially by scission of the C–O and C–N bonds, followed by further decomposition by the loss of NH_3 (aq) to form alcohols. The ¹³C NMR spectra for the decomposition products of MEA

showed peaks for methylamine, ethanol, and methanol, which is consistent with the mechanism reported by Gilbert and Lamarre⁶⁴



Likewise, the spectrum for DEA showed peaks corresponding to MEA, ethylene glycol, and methanol, which is consistent with the reaction



followed by reaction 18, along with minor peaks of other alcohols that were difficult to assign. The spectra of the decomposition products for TEA, DMEA, EAE, and 3-MPA at 350 °C and 2-DEEA at 325 °C are also not yet assigned. The main decomposition products appear to be alcohols and alkanolamines. There was no evidence of dehydration to form double bonds, as is the case for the isomers of hydroxypropanoic acid.²⁷ Because the spectra were obtained at ambient pressure, volatile decomposition products such as ethylene, methane, or CO_2 (g) would not be detected by NMR. To our knowledge, the lower thermal stability of the alkanolammonium chloride salts has not previously been reported. However, Brill and Savage⁶² have noted that increases in ionic strength support the formation of polar transition states, thereby decreasing the thermal stability of amines. The higher ionic strength of our salt solutions (0.2 – 0.8 mol kg^{-1}) would be consistent with this mechanism.

6. Conclusions

The apparent molar volume data reported here represent a considerable advance in the temperature range and number of

functional groups over the results presented by Criss and Wood⁸ in their pioneering study and subsequent studies by ourselves and other workers that for the most part do not extend to temperatures above 250 °C. The simple correlation presented above is provisional, because it is based on measurements for a very limited number of organic solutes. Nevertheless, the model differentiates between the three alkyl functional groups, ($-\text{CH}_3$), ($>\text{CH}_2$) and ($>\text{CH}-$), and includes the ($>\text{NH}$) and ($\geq\text{N}$) groups that were not described by the YSW model. The improvement over the YSW model is very significant in terms of giving the correct sign and magnitude of the divergence in V_2^0 at temperatures above 250 °C. In most cases, the model represented the experimental data to within $\pm 2 \text{ cm}^3 \cdot \text{mol}^{-1}$ at temperatures from 150 to 300 °C. It is difficult to assess the accuracy of the predictions at higher temperatures because of uncertainties in determining whether decomposition reactions had taken place for compounds that might have formed volatile reaction products; however, in most cases the accuracy probably lies within $\pm 5 \text{ cm}^3 \cdot \text{mol}^{-1}$ at temperatures from 300 to 310 °C. The data base is very limited and although it is sufficient to analyze trends, reliable values of V_2^0 are needed for many more systems for comparison on the region beyond 300 °C. The YSW and other functional group additivity models contain appropriate terms for representing complex hydration behavior near ambient conditions, which have been omitted from our treatment, and no doubt could be extended to cover a wider range in temperature by including the new data. Both the YSW model and our model performed poorly in predicting the V_2^0 of tartaric acid, glycolic acid, and 1,2,3-propanetriol. There would presumably be similar problems with other compounds having closely spaced polar groups. Future improvements of the method might result from including a dipole moment correction term, formulating an improved equation of state, and measuring a much larger set of data if enough thermally stable compounds can be identified.

Finally, we note that Plyasunov et al.⁷ and Plyasunov and Shock^{65,66} have reported methods for estimating the Krichevskii parameter by extrapolating a variety of thermodynamic functions from lower temperatures up to the limiting near-critical condition described by eq 10. The significant changes in functional group additivity parameters in the range 250 to 300 °C, shown in Figure 7, suggest that data at temperatures above 300 °C are required to make such extrapolations reliably.

Acknowledgment. This work was supported by the Natural Sciences and Engineering Research Council of Canada (NSERC) and the University of Guelph. We are grateful to the Chemistry/Physics Machine Shop at the University of Guelph for maintaining the high-temperature densimeter. We thank Professor John Goddard for helpful discussions and advice on the quantum mechanical calculations with *Gaussian 03* and Professor Andy Hakin of the University of Lethbridge who was external examiner for the Dr. Bulemela's Ph.D. thesis, on which much of this paper is based.

References and Notes

- (1) Mesmer, R. E.; Marshall, W. L.; Palmer, D. A.; Simonson, J. M.; Holmes, H. F. *J. Solution Chem.* **1988**, *27*, 699–718.
- (2) Tanger, J. C.; Helgeson, H. C. *Am. J. Sci.* **1988**, *288*, 19–98.
- (3) Shock, E. L.; Helgeson, H. C. *Geochim. Cosmochim. Acta* **1990**, *54*, 915–945.
- (4) Sedlbauer, J.; O'Connell, J. P.; Wood, R. H. *Chem. Geol.* **2000**, *163*, 43–63.
- (5) Plyasunov, A. V.; O'Connell, J. P.; Wood, R. H. *Geochim. Cosmochim. Acta* **2000**, *64*, 495–512.
- (6) Akinfiev, N. N.; Diamond, L. W. *Fluid Phase Equilib.* **2004**, *222–233*, 31–37.
- (7) Plyasunov, A. V.; Shock, E. L.; O'Connell, J. P. *Fluid Phase Equilib.* **2006**, *247*, 18–31.
- (8) Criss, C. M.; Wood, R. H. *J. Chem. Thermodyn.* **1996**, *28*, 723–741.
- (9) Amend, J. P.; Helgeson, H. C. *Geochim. Cosmochim. Acta* **1997**, *61*, 11–46.
- (10) Yezdimer, E. M.; Sedlbauer, J.; Wood, R. H. *Chem. Geol.* **2000**, *164*, 259–280.
- (11) Tremaine, P. R.; Shvedov, D.; Xiao, C. *J. Phys. Chem.* **1997**, *101*, 409–419.
- (12) Shvedov, D.; Tremaine, P. R. *J. Solution Chem.* **1997**, *26*, 1113–1142.
- (13) Hawrylak, B.; Palepu, R.; Tremaine, P. R. *J. Chem. Thermodyn.* **2006**, *38*, 988–1007.
- (14) Levelt Sengers, J. M. H. In *Supercritical Fluid Technology: Reviews in Modern Theory and Applications*; Bruno, T. J., Ely, J. F., Eds.; CRC Press: Boca Raton, FL, 1991; Chapter 1.
- (15) O'Connell, J. P.; Liu, H. *Fluid Phase Equilib.* **1998**, *144*, 1–12.
- (16) Clarke, R. G.; Tremaine, P. R. *J. Phys. Chem. B* **1999**, *103*, 5131–5137.
- (17) Clarke, R. G.; Hnědkovský, L.; Tremaine, P. R.; Majer, V. *J. Phys. Chem. B* **2000**, *104*, 11781–11793.
- (18) Balakrishnan, P. V. *J. Solution Chem.* **1988**, *17*, 825–840.
- (19) Majer, V.; Sedlbauer, J.; Hnědkovský, L.; Wood, R. H. *Phys. Chem. Chem. Phys.* **2000**, *2*, 2907–2917.
- (20) Hynčica, P.; Hnědkovský, L.; Cibulka, I. *J. Chem. Thermodyn.* **2004**, *36*, 1095–1103.
- (21) Albert, H. J.; Wood, R. H. *Rev. Sci. Instrum.* **1984**, *55*, 589–593.
- (22) Corti, H. R.; Fernández-Prini, R.; Svarc, F. *J. Solution Chem.* **1990**, *19*, 793–809.
- (23) Xiao, C.; Bianchi, H.; Tremaine, P. R. *J. Chem. Thermodyn.* **1997**, *29*, 261–286.
- (24) Hill, P. G. *J. Phys. Chem. Ref. Data* **1990**, *19*, 1233–1274.
- (25) Archer, D. G. *J. Phys. Chem. Ref. Data* **1992**, *21*, 793–829.
- (26) Bulemela, E.; Tremaine, P. R. *J. Phys. Chem. B* **2005**, *109*, 20539–20545.
- (27) Bulemela, E.; Tremaine, P. R. *J. Solution Chem.* **2007**, *36*, 1525–1546.
- (28) Young, T. F.; Smith, M. B. *J. Phys. Chem.* **1954**, *58*, 716–724.
- (29) Shock, E. L.; Helgeson, H. C. *Geochim. Cosmochim. Acta* **1988**, *52*, 2009–2036.
- (30) Johnson, J. W.; Oelkers, E. H.; Helgeson, H. C. *Comput. Geosci.* **1992**, *18* (7), 899–947.
- (31) Schulte, M. D.; Shock, E. L.; Obšil, M.; Majer, V. *J. Chem. Thermodyn.* **1999**, *31*, 1195–1229.
- (32) Majer, V.; Sedlbauer, J.; Wood, R. H. In *Aqueous Systems at Elevated Temperatures and Pressures: Physical Chemistry in Water, Steam, and Aqueous Solutions*; Palmer, D. A., Fernandez-Prini, R., Harvey, A. H., Eds.; Elsevier Academic Press: Amsterdam, The Netherlands, 2004; Chapter 4.
- (33) Sharygin, A. V.; Wood, R. H. *J. Chem. Thermodyn.* **1997**, *29*, 125–148.
- (34) Archer, D. G.; Wang, P. *J. Phys. Chem. Ref. Data* **1990**, *19*, 371–411.
- (35) Shock, E. L.; Oelkers, E. H.; Johnson, J. W.; Sverjensky, D. A.; Helgeson, H. C. *J. Chem. Soc., Faraday Trans.* **1992**, *88*, 803–826.
- (36) DiGulio, R. M.; Lee, R. J.; Schaeffer, S. T.; Brasher, L. L.; Teja, A. S. *J. Chem. Eng. Data* **1992**, *37*, 239–242.
- (37) (a) Cabani, S.; Mollica, V.; Lepori, L.; Lobo, S. T. *J. Phys. Chem.* **1977**, *81*, 987–993; (b) Cabani, S.; Matteoli, E.; Selli, E. *J. Chem. Soc., Faraday Trans. 1* **1979**, *75*, 363–369.
- (38) Maham, Y.; Teng, T. T.; Hepler, L. G.; Mather, A. E. *J. Solution Chem.* **1994**, *23*, 195–205.
- (39) Maham, Y.; Teng, T. T.; Mather, A. E.; Hepler, L. G. *Can. J. Chem.* **1995**, *73*, 1514–1519.
- (40) Maham, Y.; Teng, T. T.; Hepler, L. G.; Mather, A. E. *Thermochim. Acta* **2002**, *386*, 111–118.
- (41) Hawrylak, B.; Burke, S. E.; Palepu, R. *J. Solution Chem.* **2000**, *29*, 575–594.
- (42) Collins, C.; Tobin, J.; Shvedov, D.; Palepu, R.; Tremaine, P. R. *Can. J. Chem.* **2000**, *78*, 151–165.
- (43) Zhang, F. Q.; Li, H. P.; Dai, M.; Zhao, J. P. *Thermochim. Acta* **1995**, *254*, 347–357.
- (44) LeBrette, L.; Maham, Y.; Teng, T. T.; Hepler, L. G.; Mather, A. E. *Thermochim. Acta* **2002**, *386*, 119–126.
- (45) Lampreia, I. M. S.; Dias, F. A.; Mendonça, Â. F. S. *Phys. Chem. Chem. Phys.* **2003**, *5*, 4869–4874.
- (46) Barbas, M. J. A.; Dias, F. A.; Mendonça, Â. F. S. S.; Lampreia, I. M. S. *Phys. Chem. Chem. Phys.* **2000**, *2*, 4858–4863.
- (47) Maham, Y.; Hepler, L. G.; Mather, A. E.; Hakin, A. W.; Marriott, R. A. *J. Chem. Soc., Faraday Trans.* **1997**, *93* (9), 1747–1750.

- (48) Ben-Naim A. *Solvation Thermodynamics*; Plenum Press: New York, 1987.
- (49) Beveridge, D. L.; Schnuelle, G. W. *J. Phys. Chem.* **1975**, *79*, 2562–2566.
- (50) O'Connell, J. P. *Fluid Phase Equilib.* **1995**, *104*, 21–39.
- (51) Inglese, A.; Sedlbauer, J.; Yezdimer, E. M.; Wood, R. H. *J. Chem. Thermodyn.* **1997**, *29*, 517–531.
- (52) O'Connell, J. P.; Sharygin, A. V.; Wood, R. H. *Ind. Eng. Chem. Res.* **1996**, *35*, 2808–2812.
- (53) Hynčica, P.; Hnědkovský, L.; Cibulka, I. *J. Chem. Thermodyn.* **2006**, *38*, 1085–1091.
- (54) Hynčica, P.; Hnědkovský, L.; Cibulka, I. *J. Chem. Thermodyn.* **2006**, *38*, 801–809.
- (55) Hynčica, P.; Hnědkovský, L.; Cibulka, I. *J. Chem. Thermodyn.* **2006**, *38*, 418–426.
- (56) Cibulka, I.; Hnědkovský, L.; Hynčica, P. *J. Mol. Liq.* **2007**, *131–132*, 206–215.
- (57) Lepori, L.; Gianni, P. *J. Solution Chem.* **2000**, *29*, 405–447.
- (58) Quint, J. R.; Wood, R. H. *J. Phys. Chem.* **1985**, *89*, 380–384.
- (59) Lin, S. T.; Sandler, S. I. *Chem. Eng. Sci.* **2002**, *57*, 2727–2733.
- (60) Seward T. M.; Driesner, T. In *Aqueous Systems at Elevated Temperatures and Pressures: Physical Chemistry in Water, Steam, and Aqueous Solutions*; Palmer, D. A., Fernandez-Prini, R., Harvey, A. H., Eds.; Elsevier Academic Press: Amsterdam, The Netherlands, 2004; Chapter 5.
- (61) Thakkar, A. J.; Kassimi, N. E.; Hu, S. *Chem. Phys. Lett.* **2004**, *387*, 142–148.
- (62) Brill, T. B.; Savage, P. E. In *Aqueous Systems at Elevated Temperatures and Pressures: Physical Chemistry in Water, Steam, and Aqueous Solutions*; Palmer, D. A., Fernandez-Prini, R., Harvey, A. H., Eds.; Elsevier Academic Press: Amsterdam, The Netherlands, 2004; Chapter 16.
- (63) Katritzky, A. R.; Nichols, D. A.; Sinkin, M.; Murugan, R.; Balasubramanian, M. *Chem. Rev.* **2001**, *101*, 837–892.
- (64) Gilbert, R.; Lamarre, C. *J. Chem. Eng.* **1989**, *67*, 646–651.
- (65) Plyasunov, A. V.; Shock, E. L. *J. Supercritical Fluids* **2001**, *20*, 91–103.
- (66) Plyasunov, A. V.; Shock, E. L. *Fluid Phase Equilib.* **2004**, *222–223*, 19–24.